



Geological Survey Paper 12: Structural Geology of the Red Point Metamorphic Complex, Southern Tyennan Domain, Tasmania

Author: D. R. Gray and M. J. Vicary
Date: 25/10/2022
Email: info@mrt.tas.gov.au
Website: www.mrt.tas.gov.au

REPORT No.: GSP12



Red Point Hills and Red Point Peninsula with Cox Bight in foreground. Aerial view looking to the southeast showing rock platform outcrops along the eastern side of Cox Bight to Bridge Point with Maatsuyker Island in the distance (photo right). The southern end of the Red Point Hills (middle left) slopes gradually to towards Red Point. The Red Point Metamorphic Complex consists of two outcrop belts, a northern coastal remnant extending from the beach south to the first embayment and a southern belt from Contact Cove to Red Point (the last visible part of the coastline shadowed by Walker and Maatsuyker Islands on the horizon). The intervening coastal outcrops are in low-grade pelite that makes up the Red Point Hills.



Mineral Resources Tasmania
mrt

Contents

1.0 INTRODUCTION	3
2.0 BACKGROUND	7
2.1 Mapping.....	7
2.2 Protolith and Provenance.....	8
2.3 Metamorphism.....	8
2.4 Current Compilation.....	9
3.0 STRUCTURE OF THE RED POINT METAMORPHIC COMPLEX	9
3.1 Structural Elements.....	9
3.2 Structure of the Northern High-grade Belt (NMGS).....	9
3.3 Structure of the Southern High-grade Belt (SMGS)	14
3.4 Linking the Structure of the NMGS and the SMGS.....	15
4.0 REGIONAL MAP RELATIONSHIPS/INTERPRETATION	15
5.0 SHEAR SENSE AND TRANSPORT DIRECTION FOR THE RED POINT METAMORPHIC COMPLEX.....	20
6.0 SUMMARY AND CONCLUSIONS.....	21
7.0 ACKNOWLEDGMENTS.....	22
8.0 REFERENCES	23

Abstract

The Red Point Metamorphic Complex consists of two outcrop belts of high-pressure, medium grade garnet- and porphyroblastic albite-mica-schist, quartz-mica schist and quartzite. The northern medium-grade, north-north-east-trending belt (NMGS of Mulder, 2013) and the southern medium-grade, east-northeast-trending belt (SMGS of Mulder, 2013) are in fault contact with, and separated by a low-grade sequence (LGS) consisting of laminated, locally cross-stratified quartzite and interlayered quartz-rich and biotite-white mica rich phyllite.

The NMGS and SMGS are interpreted here as the limbs of a regional scale, west-plunging, south-closing, tight to isoclinal fold cored by low-grade pelite. The hinge of the inferred macro-fold is projected offshore with the limbs represented by the NMGS north-trending belt with generalised attitude of $200^{\circ}/45^{\circ}W$ (as western limb) and the SMGS northeast-trending belt with generalised attitude of $245^{\circ}/65^{\circ}W$ (as eastern limb) giving a fold axis of $43^{\circ}/270^{\circ}$.

The Red Point Metamorphic Complex is a ~1 km thick "sheet" folded by a macro-fold with an inclined-plunging form approaching reclined geometry. This geometry is similar to that of macro-folds in the West Coast High-grade belt and in the Central Tyennan domain. The Red Point macro-fold has been obliquely refolded by younger, Devonian north-south open folding typical in the coastal exposures and in the Red Point Hills.

Younging data suggest the western, structurally higher limb (the NMGS) is structurally overturned but with right-way-up younging, whereas the southeastern structurally lower limb (the SMGS) is upside down. The axial surface trace (AST) of the macro-fold separates domains of right-way-up younging on the upper limb from upside-down younging beds on the lower limb.

It is the structurally lowest macro-fold in the Southern Tyennan domain. It sits beneath the South West Cape mega-sheath fold system but above the regional scale, asymmetric shear-lozenge made up of the S-vergent, macro-isoclinal fold-pair. The eastern Southern Tyennan domain shows 1) a reversed litho-tectonic stack of platy quartzite-quartzite-pelite-high-grade schist (top to bottom) and 2) dominantly upside-down younging from preserved cross-bedding in the low-grade quartzite sequence.

Asymmetric quartz fish and dextral shear bands in NMGS schist near the northern contact with the LGS show top-to-the east shear sense. Associated sinistral (top-to-the-west) shear bands are potentially antithetic and combined with the synthetic set give a movement plane trending $303^{\circ}-123^{\circ}$ with transport to the southeast (123°).

Structural Geology of the Red Point Metamorphic Complex, Southern Tyennan Domain, Tasmania

David R. Gray¹ and Michael J. Vicary²

¹ *Consultant Structural Geologist to Mineral Resources Tasmania*

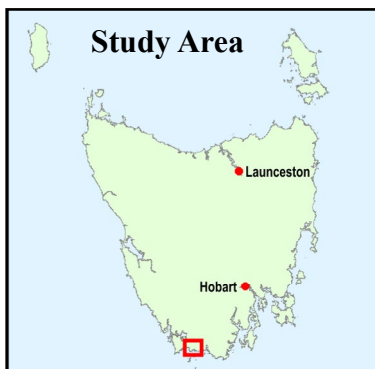
² *Geological Survey Branch - Mineral Resources Tasmania*

ARTICLE INFO

Published: xx October 2022
Publisher: Mineral Resources
Tasmania
Report No.: GSP12

KEYWORDS

Structural Geology
High-P metamorphism
Southern Tyennan



1.0 INTRODUCTION

This paper is one of a series of papers on the unique structural elements of the South Tyennan domain of South West Tasmania. It is part of the Mineral Resources Tasmania Tyennan Domain Structural Geology Series.

Structural elements of the Southern Tyennan domain (Figures 1 and 2) comprise 1) the Nye Bay fold-nappe (element 1), 2) the high-grade coastal belt isoclinal fold stack (element 2), 3) the De Witt-Propsting mega-sheath fold (element 3), 4) the Davey River sheath-fold nose (element 4), 5) the South West Cape mega-sheath fold system (element 5), 6) the S-vergent, isoclinal fold-pair "wave train" (element 6) as part of an inferred regional scale shear lozenge, and 7) the Red Point macro-fold (element 7). These stacked structural entities sit on a structurally lower, low-grade pelite/dolomitic pelite sheet (element 8).

The structural architecture of the Southern Tyennan domain presented in a schematic down-plunge profile (Figure 2) shows the stacked and complex character of this part of the Tyennan nucleus. The profile is constructed from a tilted oblique map view looking to the west.

The geometry and structural definition of the Nye Bay fold-nappe and the high-grade southwest coastal belt isoclinal fold stack (elements 1 and 2) are presented in Gray et al (2022). The geometry and structural definition of the mega-sheath fold system core of the domain (elements 3, 4 and 5) are presented in Gray and Vicary (2022b), and that of the asymmetric, isoclinal macro-fold pair (element 6), including the easternmost Arthur Range (Gray and Vicary, 2022a), are presented in Gray and Vicary (2022c).

The Red Point Metamorphic Complex (Mulder et al., 2015) occurs along the south coast of Tasmania between Cox Bight and Louisa Bay (Figures 3, 4 and 5). It consists of two blocks of high-pressure, medium-grade pelitic schist (the MGS of Mulder et al., 2015) and minor garnet-bearing amphibolite that are separated by, and faulted against, low-grade phyllite and quartzite (the LGS of Mulder et al., 2015) (Figures 4 and 5).

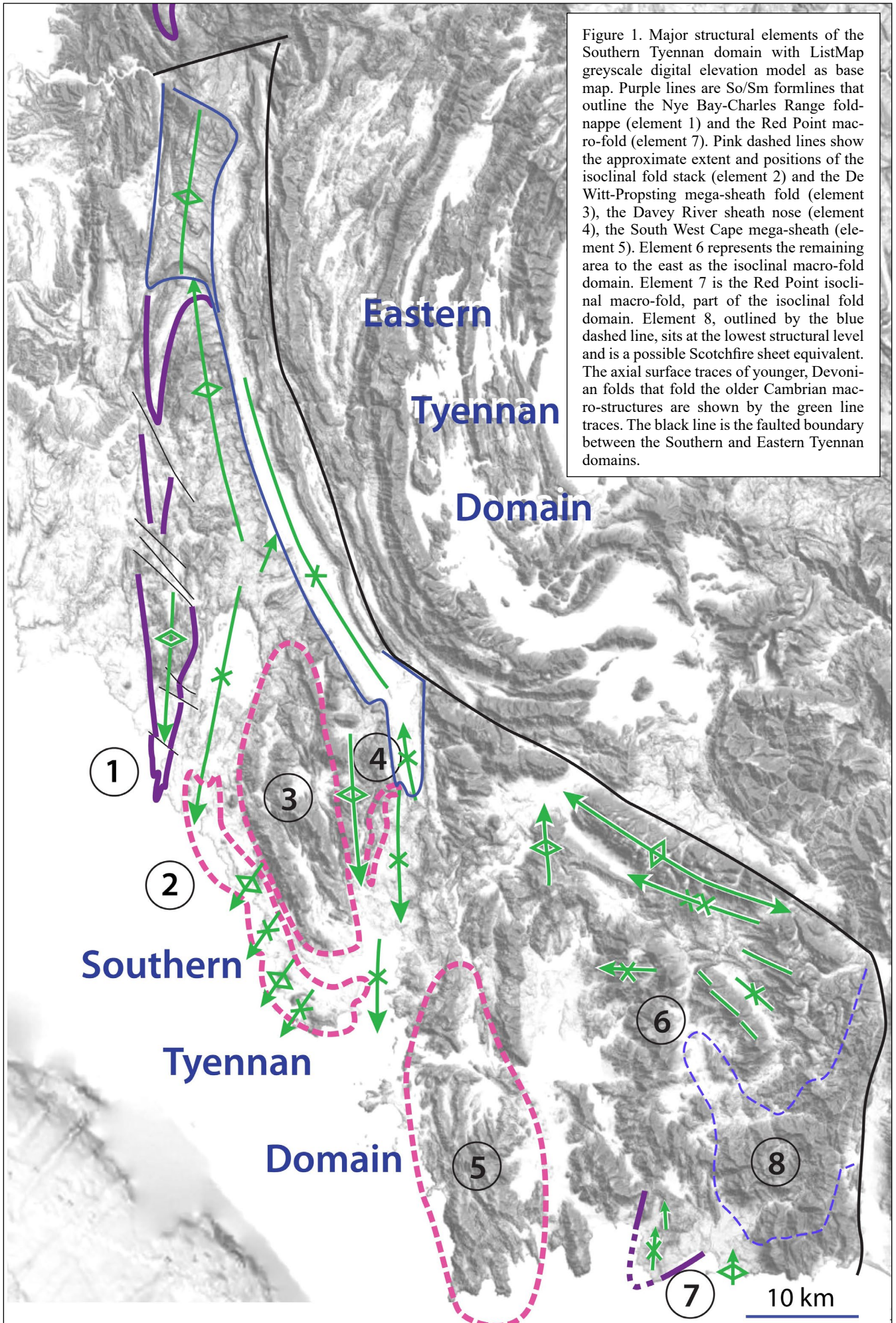


Figure 1. Major structural elements of the Southern Tyennan domain with ListMap greyscale digital elevation model as base map. Purple lines are So/Sm formlines that outline the Nye Bay-Charles Range fold-nappe (element 1) and the Red Point macro-fold (element 7). Pink dashed lines show the approximate extent and positions of the isoclinal fold stack (element 2) and the De Witt-Propsting mega-sheath fold (element 3), the Davey River sheath nose (element 4), the South West Cape mega-sheath (element 5). Element 6 represents the remaining area to the east as the isoclinal macro-fold domain. Element 7 is the Red Point isoclinal macro-fold, part of the isoclinal fold domain. Element 8, outlined by the blue dashed line, sits at the lowest structural level and is a possible Scotchfire sheet equivalent. The axial surface traces of younger, Devonian folds that fold the older Cambrian macro-structures are shown by the green line traces. The black line is the faulted boundary between the Southern and Eastern Tyennan domains.

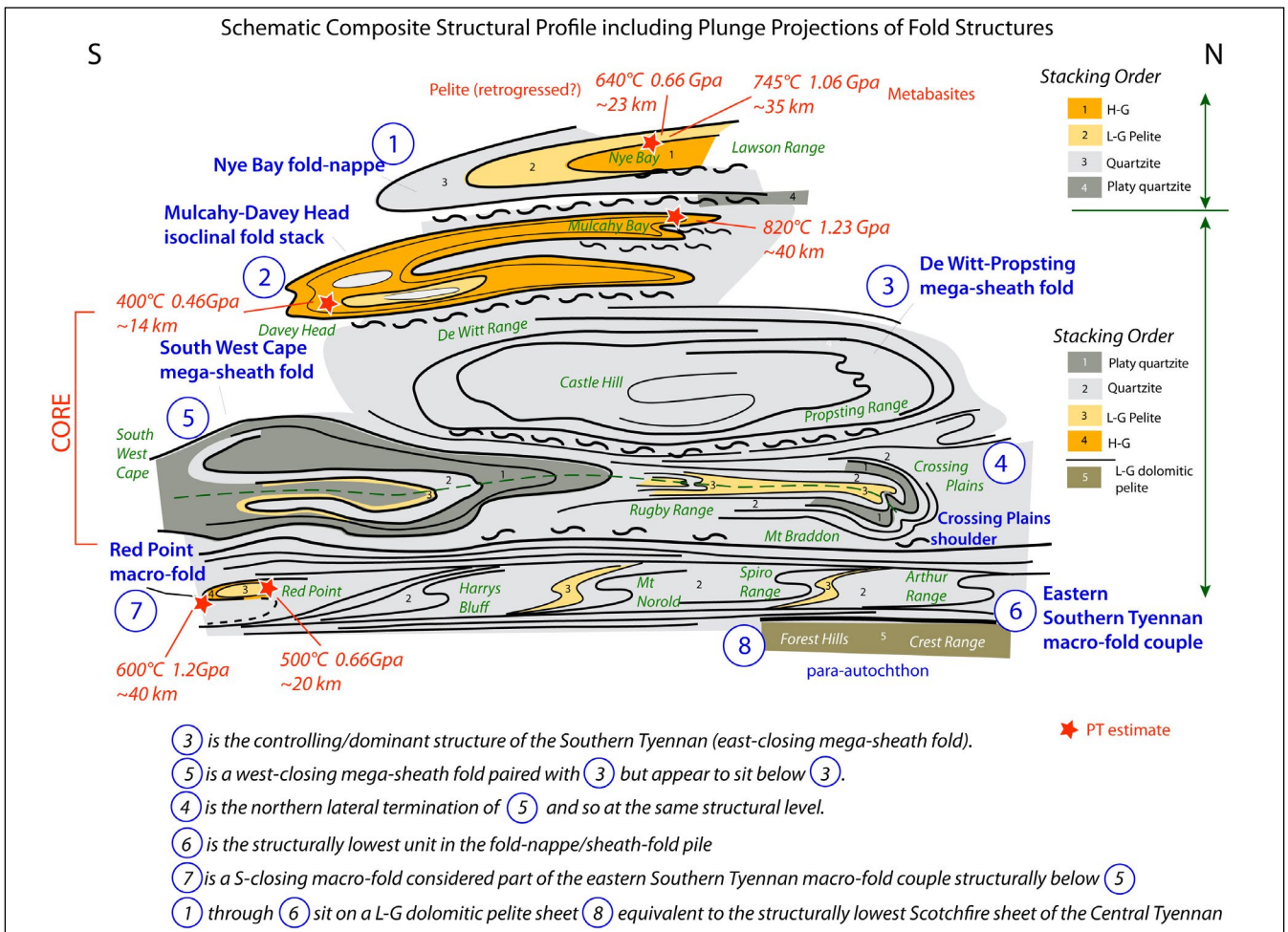


Figure 2. Schematic approximate down-plunge structural profile of the major structural elements that make up the eastern Southern Tyennan domain. The profile is a tilted map view looking to the west with north on the diagram right. The Red Point macro-fold is shown by Element 7 as part of the asymmetric, S-vergent, isoclinal macro-fold couple that dominates this part of the Southern Tyennan (element 6). The fold "wave train" occurs at the structurally lowest level and is the base of this structurally complex subducted-obducted composite sheet.

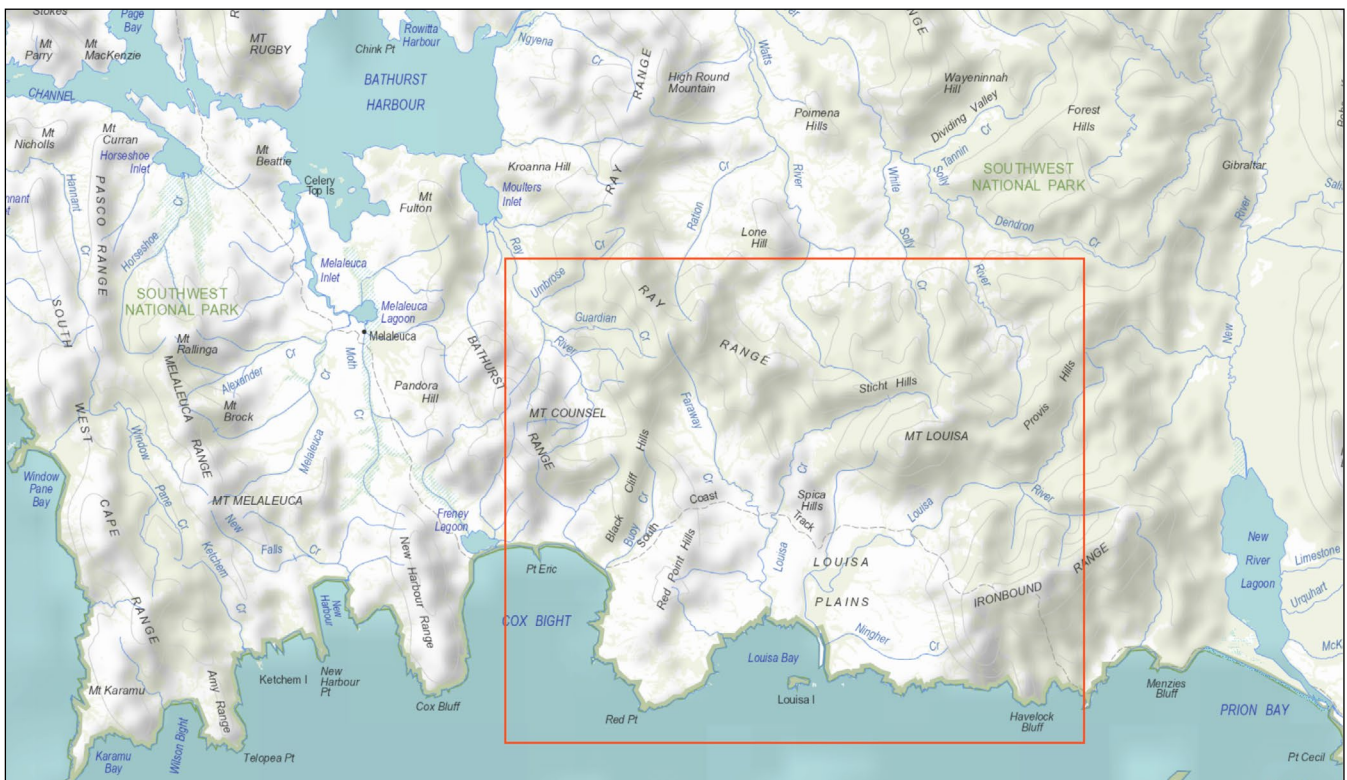


Figure 3. Tasmanian ListMap topographic map of southwest Tasmania showing mountain ranges, creeks and rivers. The Red Point study area is shown by the red rectangle.

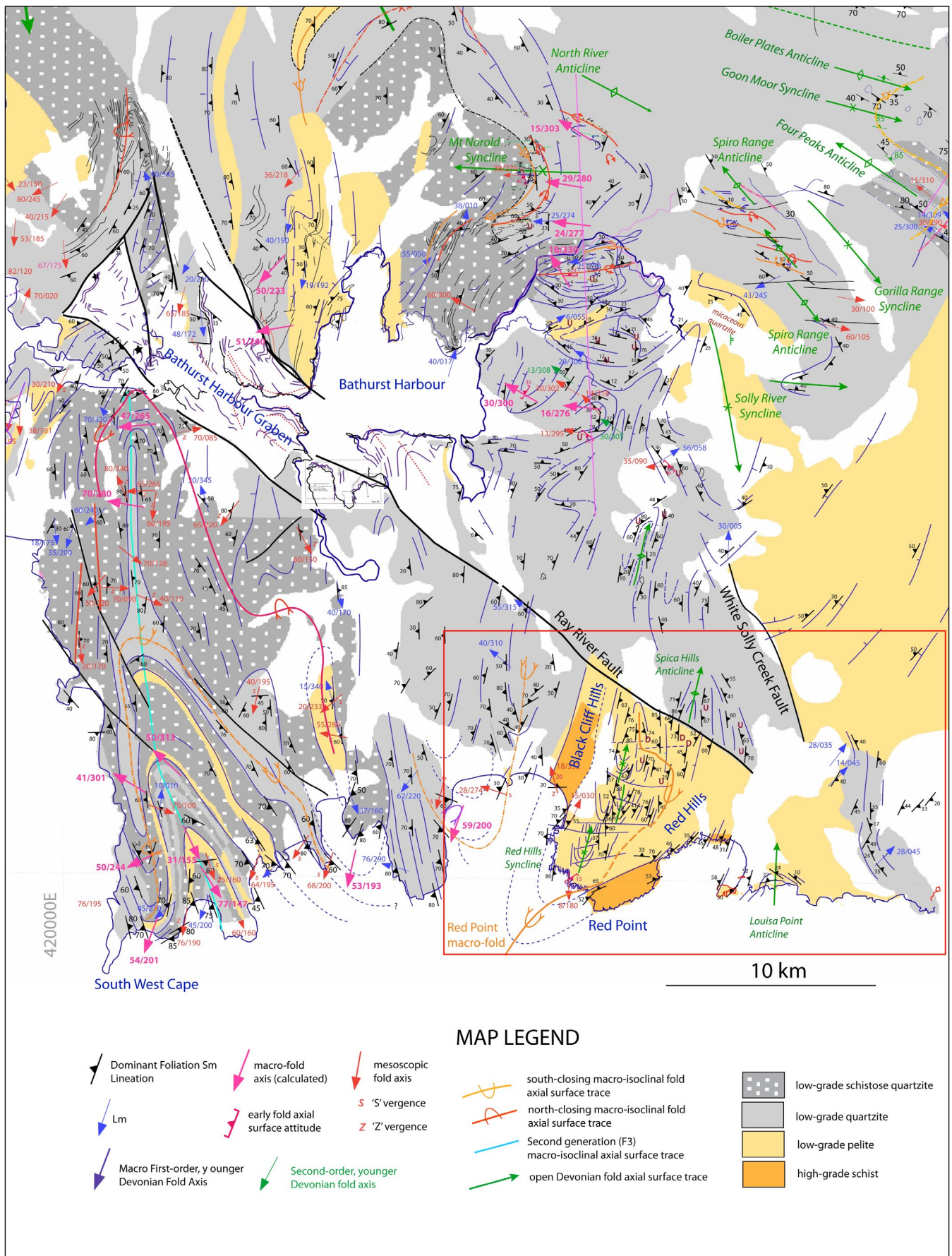


Figure 4. Structure map of the eastern part of the Southern Tyennan domain with Mineral Resources Tasmania 1:250,000 digital atlas lithological base. The structural data has been compiled from mapping by Stefanski (1957a,b), Taylor (1959), BHP geologists (Hall, 1965; Hall et al., 1969), Williams and Lennox in 1980 (Lennox, 2013), Mulder (2013) and Mulder et al. (2015).

The northern medium-grade (NMGS of Mulder, 2013) and southern medium-grade (SMGS of Mulder, 2013) sequences (Figure 5) comprise garnet and albite porphyroblastic mica-schist, quartz-mica schist and quartzite (Mulder et al., 2015). The low-grade sequence (LGS) consists of 0.1-2 m thick, laminated, locally cross-stratified quartzite and interlayered quartz-rich and biotite-white mica rich phyllite (Mulder et al., 2015).

The northern block (NMGS) is a north-northeast-trending, west-dipping slab that extends as a thin coastal strip from the northeast end of Cox Bight through Black Cliff into the Black Cliff Hills (based on mapping/lithological descriptions of Stefanski, 1957a, b) with the northern termination at the Ray River Fault. It has a slab thickness of ~1.1 km based on a strike-perpendicular outcrop width of 1.5 km and an average dip of 45°. The southern block (SMGS) is a northeast-trending, northwest-dipping slab that extends from Contact Cove to Red Point and laterally eastwards across Louisa Bay to east of Louisa Creek (based on mapping/lithological descriptions

of Lennox, 2013). It has a slab thickness of ~1.0 km based on a strike-perpendicular outcrop width of 1.2 km at an average dip of 65°.

Topographically the region consists of the Red Point Hills (elevations of 260-280 m) bounded by the Louisa Creek on the east and the Buoy Creek on the west, and rimmed by a low coastal plain (Figure 3). The northern block of schists, cut by Buoy Creek, occupies the Black Cliff Hills (elevations 300-320 m).

2.0 BACKGROUND

2.1 Mapping

Regional mapping in the Red Point Hills, the Spica Hills, Louisa Bay and the Ray Range (Figure 4) was undertaken in January-February of 1980 by Lennox (2013). Honours thesis mapping in the coastal belt from Cox Bight to Red Point was undertaken by Mulder (2013). Mesoscopic and micro-structural relationships and the metamorphic thermo-barometric calculations for the Red Point Metamorphic Complex are presented in Mulder (2013) and Mulder et al. (2015).

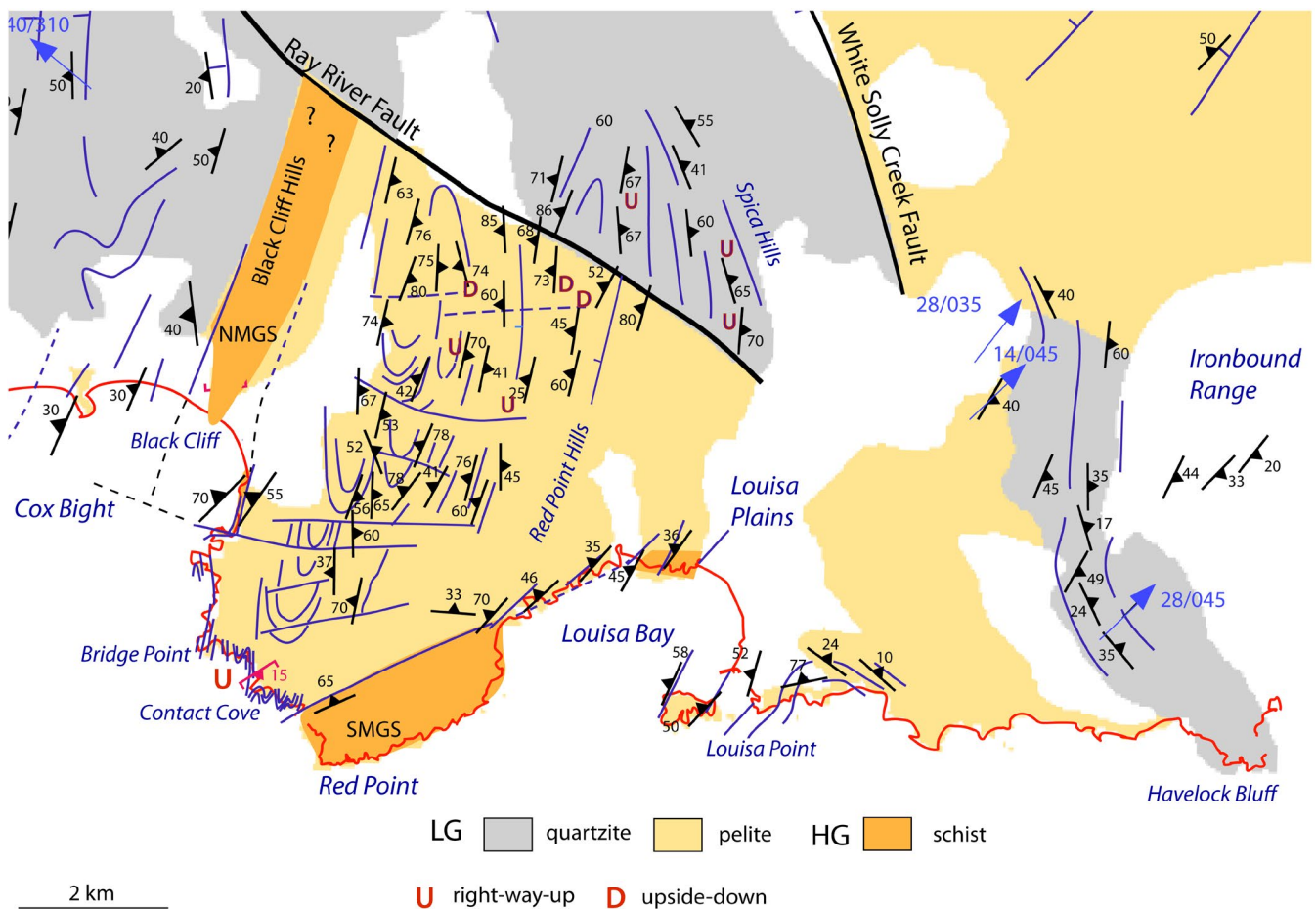


Figure 5. Structure map of the Red Point-Red Point Hills-Louisa Bay area. Structural data from 1) Lennox (2013) based on mapping in January-February of 1980, and 2) Mulder (2013) Honours thesis mapping. Younging data from Lennox (2013) plotted as D: upside down compositional layering; U: right-way-up compositional layering. Blue arrows: lineation Lm attitude data. Lithological map base is from Mineral Resources Tasmania 1:250000 digital atlas series.

NMGS: Northern medium grade sequence; SMGS: southern medium-grade sequence.

2.2 Protolith and Provenance

LGS and MGS protolith geochemistry (Mulder, 2013) suggest lithologies are a combination of continental-derived siliciclastic sediments and tholeiitic basalts, with amphibolites having MORB affinity (Meffre et al., 2000; Mulder et al., 2015).

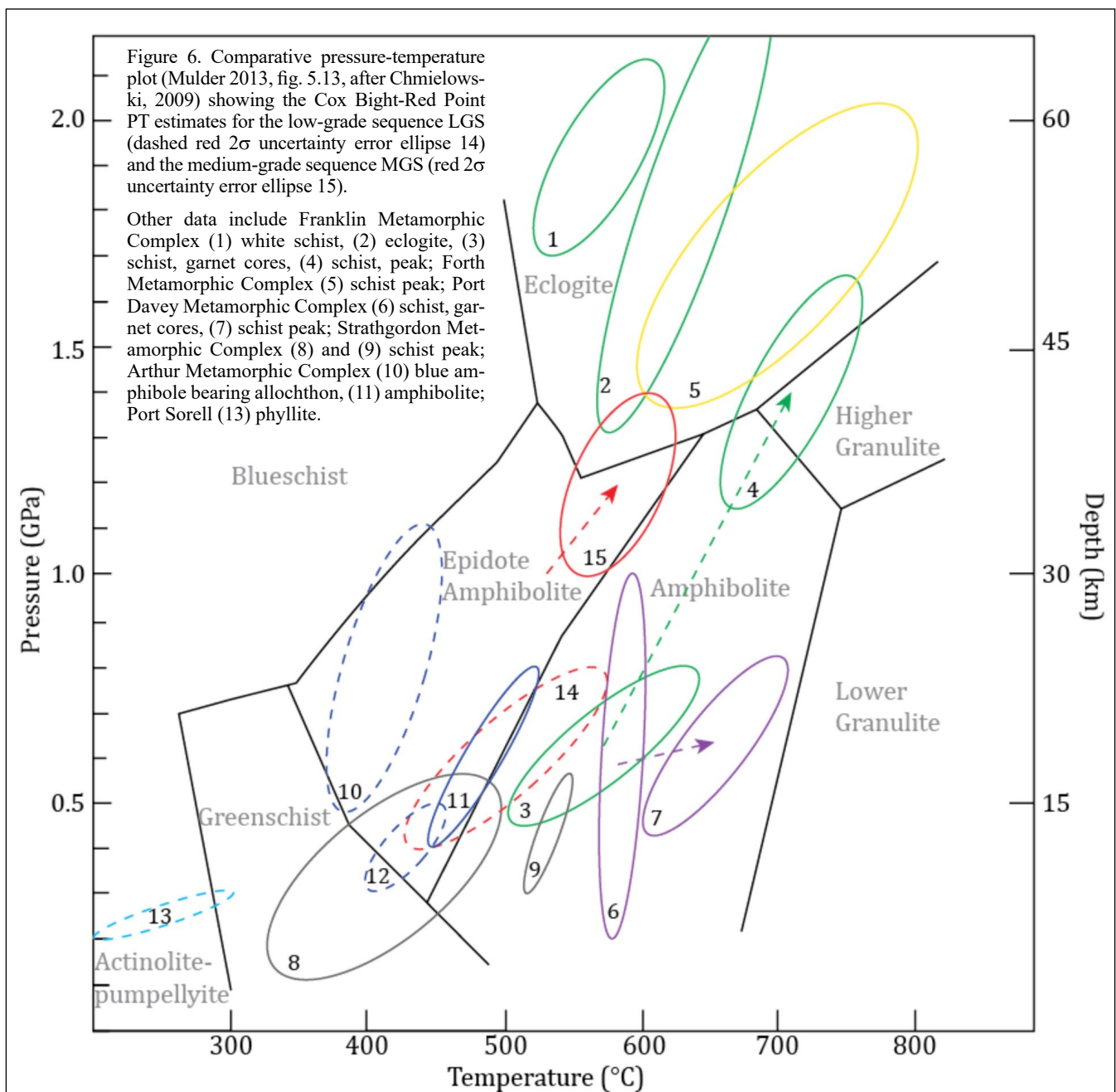
Detrital zircon population analysis (Mulder, 2013), despite small zircon populations, show that both the MGS (n=64) and LGS (n=54) have remarkable similarity in detrital zircon populations, reflected by the size and distribution of individual modes. This suggests that 1) MGS and LGS source regions were not far removed from each other, and 2) MGS and LGS sediments had a similar provenance. Further, comparison with other data (Halpin et al., 2014) suggests they equate to zircon populations of the lower Rocky Cape Group (Mulder, 2013, fig.7.2).

2.3 Metamorphism

Peak metamorphic conditions for the Red Point Metamorphic Complex (Mulder et al., 2015) are:

- **LGS** (biotite and Kspar rich bands): ~500°C and 0.6 GPa
- **MGS** (garnet): ~600°C and ~1.2 GPa, followed by isothermal decompression (Figure 6).

In both the MGS and LGS sequences the peak metamorphic conditions (Figure 6) were synchronous with development of a pervasive schistosity S_m and meso-scale isoclinal folds (Mulder et al., 2015). Schistosity development occurred by complete transposition of S_2 into a continuous fabric. The later stages of S_2 growth post-date the peak metamorphic conditions with the breakdown of garnet suggesting decompression along the retrograde path (Mulder et al., 2015). Curvature of inclusion trails towards the rims of albite porphyroblasts suggest that albite either grew continuously or episodically during the later stages of S_2 growth.



The different peak metamorphic conditions for the medium grade (MGS) and low-grade (LGS) sequences suggest that they are exhumed slices derived from different levels within the former subducted continental during the middle Cambrian arc-continent collisional event (Mulder et al., 2015).

2.4 Current Compilation

The current work is a synthesis utilising structural data from Lennox (2013) and Mulder (2013) in an attempt to 1) put the Red Point Metamorphic Complex into a regional context, and 2) define and explain the position of the Red Point Metamorphic Complex in the overall regional structure of the Southern Tyennan domain.

The work is presented as a series of maps and structural profiles with a resulting 3D geometric interpretation of the Red Point region. No fieldwork or field checking has been done by the authors and hence many of the figures and photos are adapted from or taken from Mulder (2013) or Mulder et al. (2015).

All map grids and grid references in the text have a GDA94 datum with MGA coordinates in Zone 55.

All structural data utilised and/or presented are true north unless otherwise stated.

The following **structural terminology** is used:

So/Sm	metamorphic foliation parallel to bedding (commonly a transposition layering)
So/Sm env	enveloping surface to folded So/Sm
Sm	dominant or main metamorphic foliation
Sb	shear band (S-C' structure)
AST	fold axial surface trace
AS/Sm	dominant foliation sub-parallel to fold axial surfaces
Sm/Sb	dominant foliation developing from Sb, shear band foliation
Sc	crenulation cleavage
Sc1	Devonian overprinting low-grade cleavage
S1	early slaty cleavage
Lm	dominant lineation
Lstretch	stretching lineation
Lelongation	mineral elongation lineation
TD	transport direction
Lint	intersection lineation
Lrod	rodding lineation developed from deforming Lint
FA	fold axis
F1, F2, F3	local age of fold axes (oldest to youngest)
Lm^FA	angle between Lm and FA
Sm^Sb	angle between Sm and Sb

3.0 STRUCTURE OF THE RED POINT METAMORPHIC COMPLEX

3.1 Structural Elements

Early F1/F2 tight-isoclinal mesoscopic folds fold the compositional layering in all lithologies (Figures 7, 8 and 9). The wavelengths of the folds are up to 2-3 m in the quartzite dominant package (Figure 7) and generally 20-50 cm in the phyllites and medium grade schists (Figures 8 and 9) (Mulder, 2013). They have an associated axial surface foliation in the low-grade phyllites that is a pervasive schistosity in the high-grade schist sequences (Figures 10 and 11).

The dominant schistosity Sm in the high-grade schists is an intense transposition foliation designated S2 by Mulder (2013) based on microstructure (Figures 10 and 11). An earlier layering (So/S1) is rarely preserved as isoclinal hinges in some quartz-rich microlithons and as internal inclusion tails (Si) within albite porphyroblasts discordant to the external foliation (Se) (Figure 11).

Younger upright, north-south-trending, open folds (designated as F3 by Mulder, 2013) refold both compositional layering and the early isoclinal folds (Figure 9). These folds dominate the coastal outcrops between Bridge Point and Contact Cove (Figure 5) and are part of the more regional-scale folds that define the structure of the Red Point Hills (Figure 5).

3.2 Structure of the Northern High-grade Belt (NMGS)

The northern outcrop belt is north trending and moderately to steeply west-dipping. It is truncated and/or bounded in the south by an east-northeast-trending high strain zone. The NMGS and the bounding high strain zone are cut and offset by steep, brittle, northwest-trending dextral strike-slip faults (Figure 12). Mica schist at the interface is totally disrupted with quartz ribbons (Figure 13). Compositional layering (So/Sm) in the low-grade rocks is sub-parallel to the contact in a 15-20 m zone (Figure 12), with a suggestion of shear bands just below the litho-tectonic contact (Figure 12b and 14).

Transposed layering occurs in both the NMGS (Figure 13) and the LGS but there is a significant brittle overprint with 1) sharp, discrete northwest-dipping, normal sense fault planes and 2) zones of cataclasis with phacoids of LGS within disrupted NMGS mica schist (Mulder, 2013, fig. 3.5). The contact is a zone of later reactivation with at least two sets of brittle faults (Mulder et al., 2015) including 1) contact parallel, northwest-dipping, normal-sense, brittle faults (fig. 3.5, Mulder, 2013) and 2) sub-vertical northwest- and east-west trending strike-slip faults with apparent dextral sense (Figure 12).



Figure 7. Flattened, isoclinal early F1/F2 fold in quartzite sequence of the low-grade quartzite sequence east of Bridge Point. (photo fig. 3.6c, Mulder, 2013).

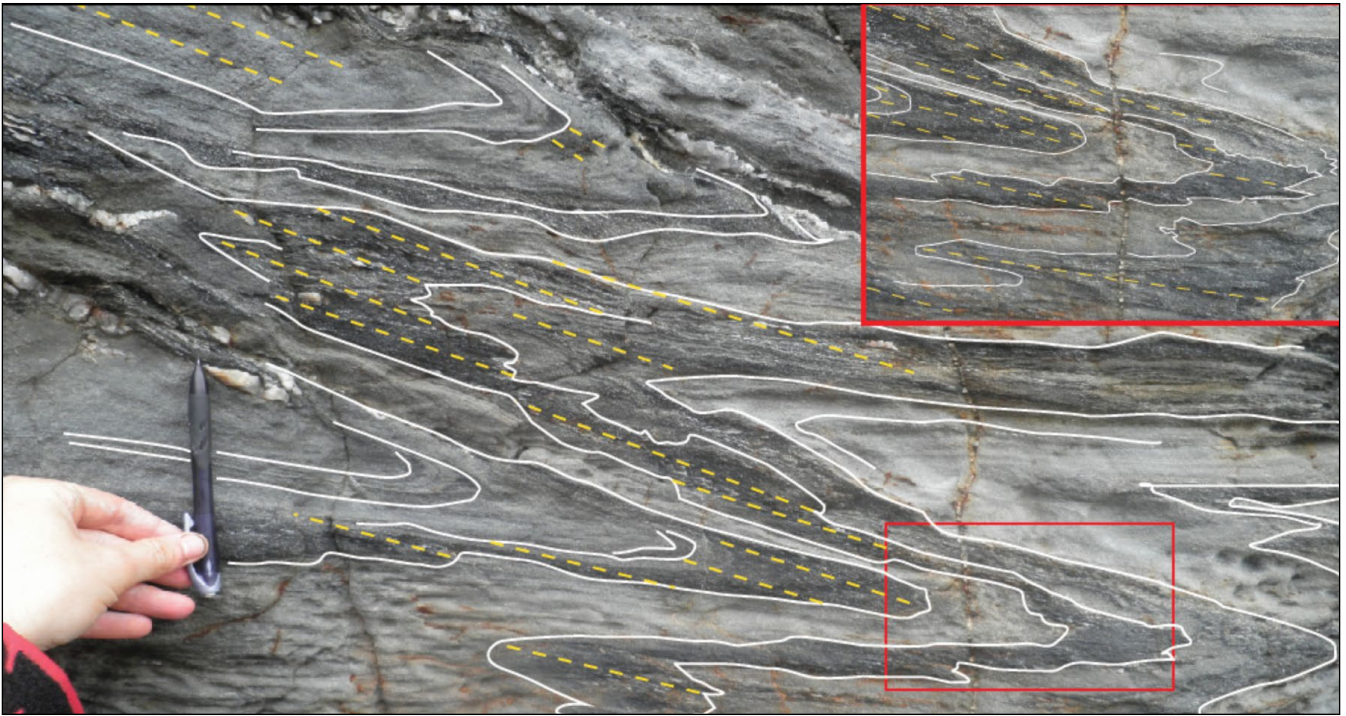


Figure 8. Isoclinal early F1/F2 folds in the northern high-grade belt (NMGS) showing strongly developed axial planar schistosity (yellow dashed lines) (fig. 4b, Mulder et al., 2015). The inset (top right corner) is an enlargement of the hinge area outlined by the red rectangle (photo lower right).

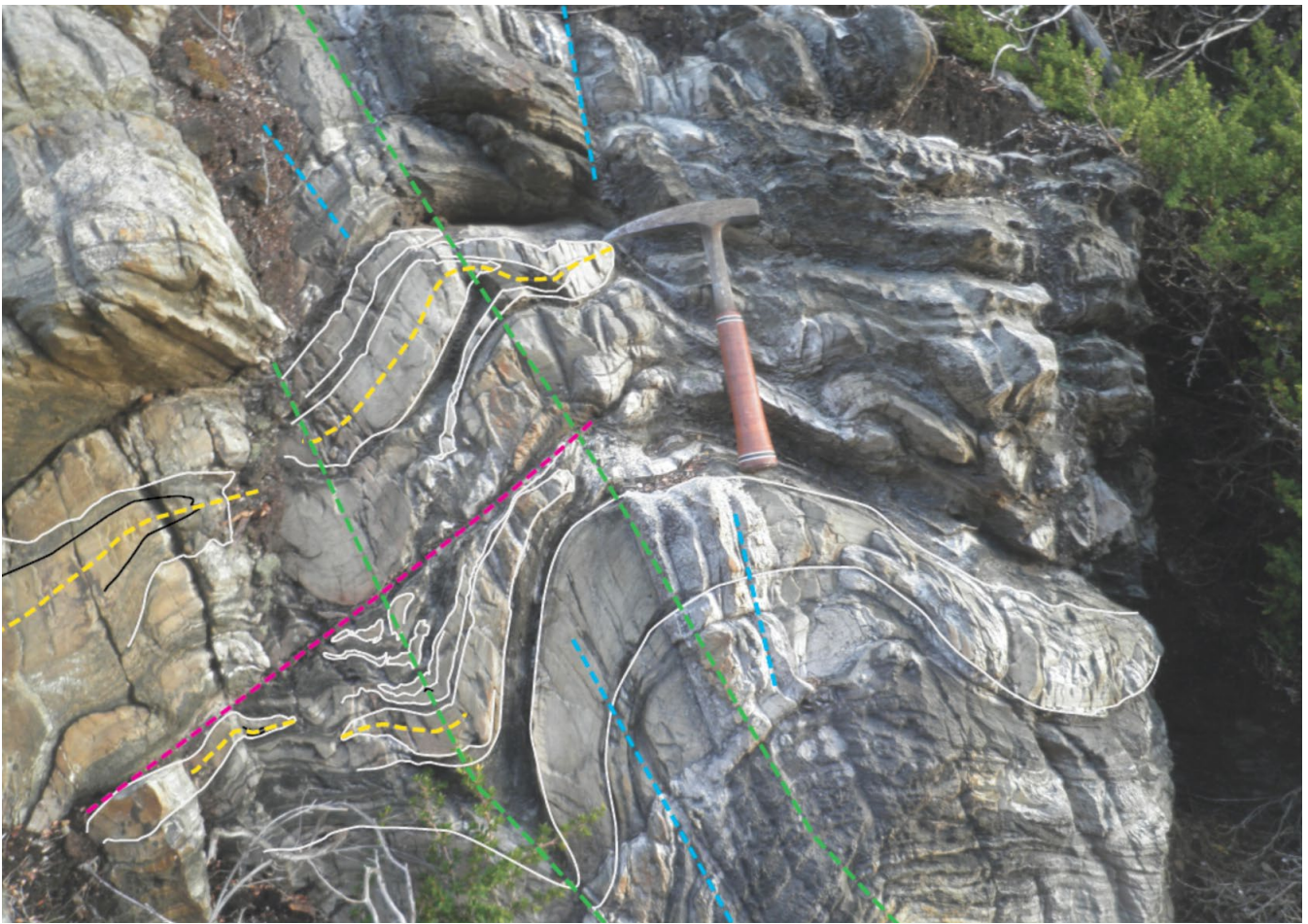


Figure 9. Approximately recumbent, isoclinal meso-fold hinges (yellow dashed lines as axial surface traces) and some closed loops (centre-left) indicating sheath-like character with curved hingelines (fig. 4d, Mulder et al., 2015). These early isoclinal folds are refolded by upright, open north-south trending folds (axial traces as green dashed lines).

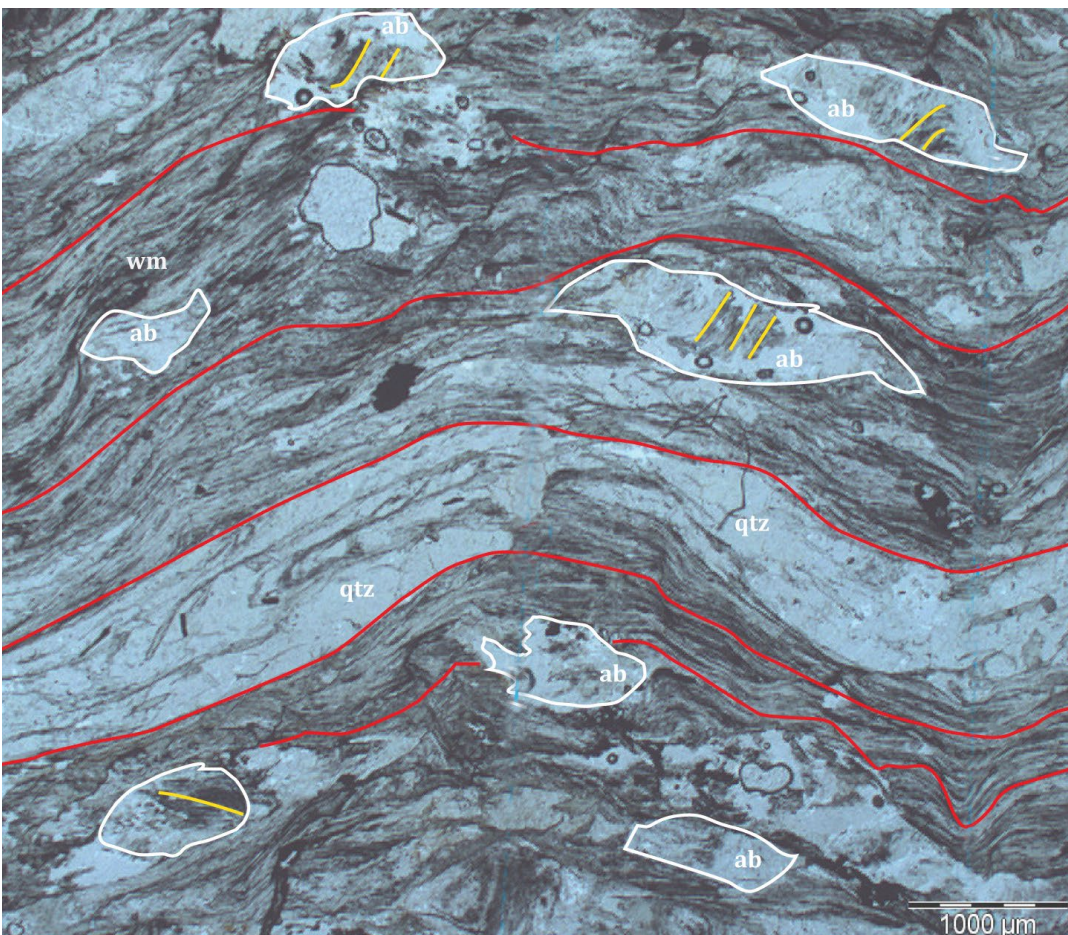


Figure 10. Dominant schistosity S_m (red lines) defined by alternating mica-rich and quartz-rich layering (fig. 5e, Mulder et al., 2015). wm: white mica; qtz: quartz; ab: albite. Yellow line traces: internal foliation (S_i) within the porphyroblasts.

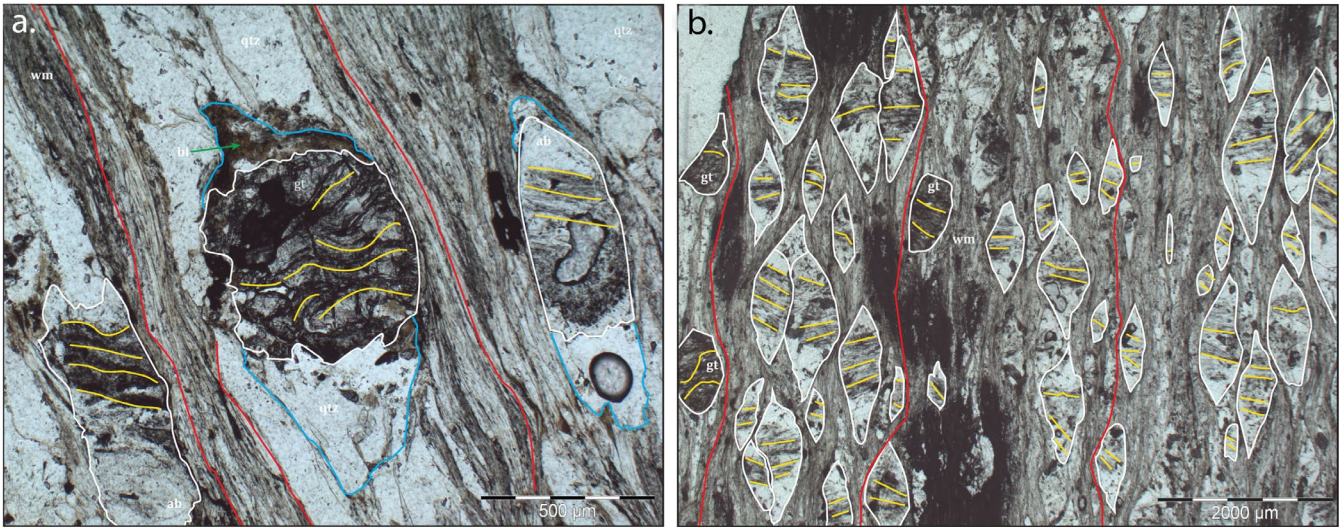


Figure 11. Dominant schistosity S2 fabric relationships. a) Intense transposition layering defined by alternating zones of white mica (wm) and quartz (qtz) enclosing garnet and albite with quartz ± biotite pressure shadow growths (fig. 5a, Mulder et al., 2015). b) Dominant foliation as intense mica alignment defining schistosity in pelitic schist enclosing canoe-shaped albite porphyroblasts with quartz overgrowths as tails (fig. 5d, Mulder et al., 2015).

Red line traces: dominant foliation Sm; yellow line traces: internal foliation (Si) within the porphyroblasts.

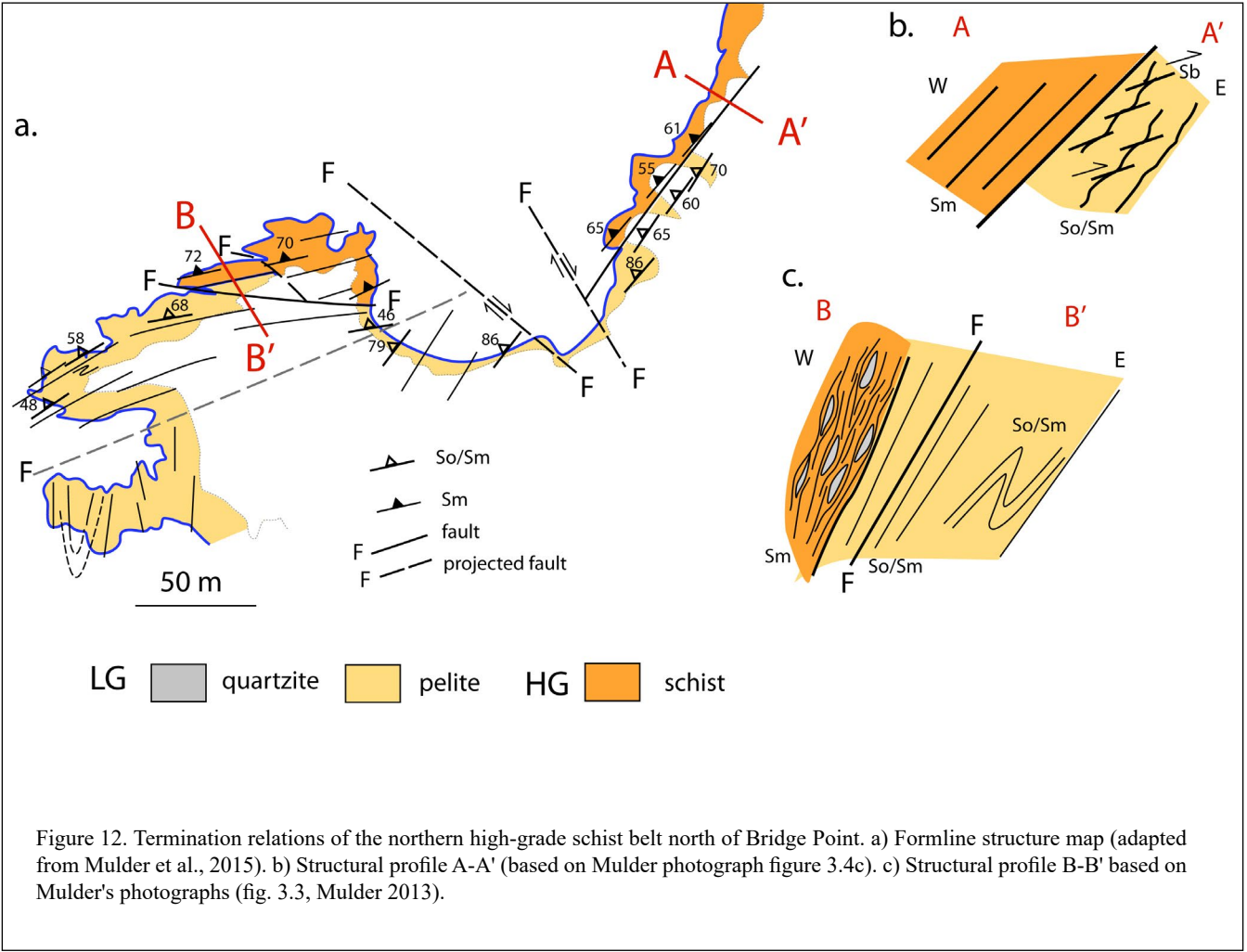


Figure 12. Termination relations of the northern high-grade schist belt north of Bridge Point. a) Formline structure map (adapted from Mulder et al., 2015). b) Structural profile A-A' (based on Mulder photograph figure 3.4c). c) Structural profile B-B' based on Mulder's photographs (fig. 3.3, Mulder 2013).

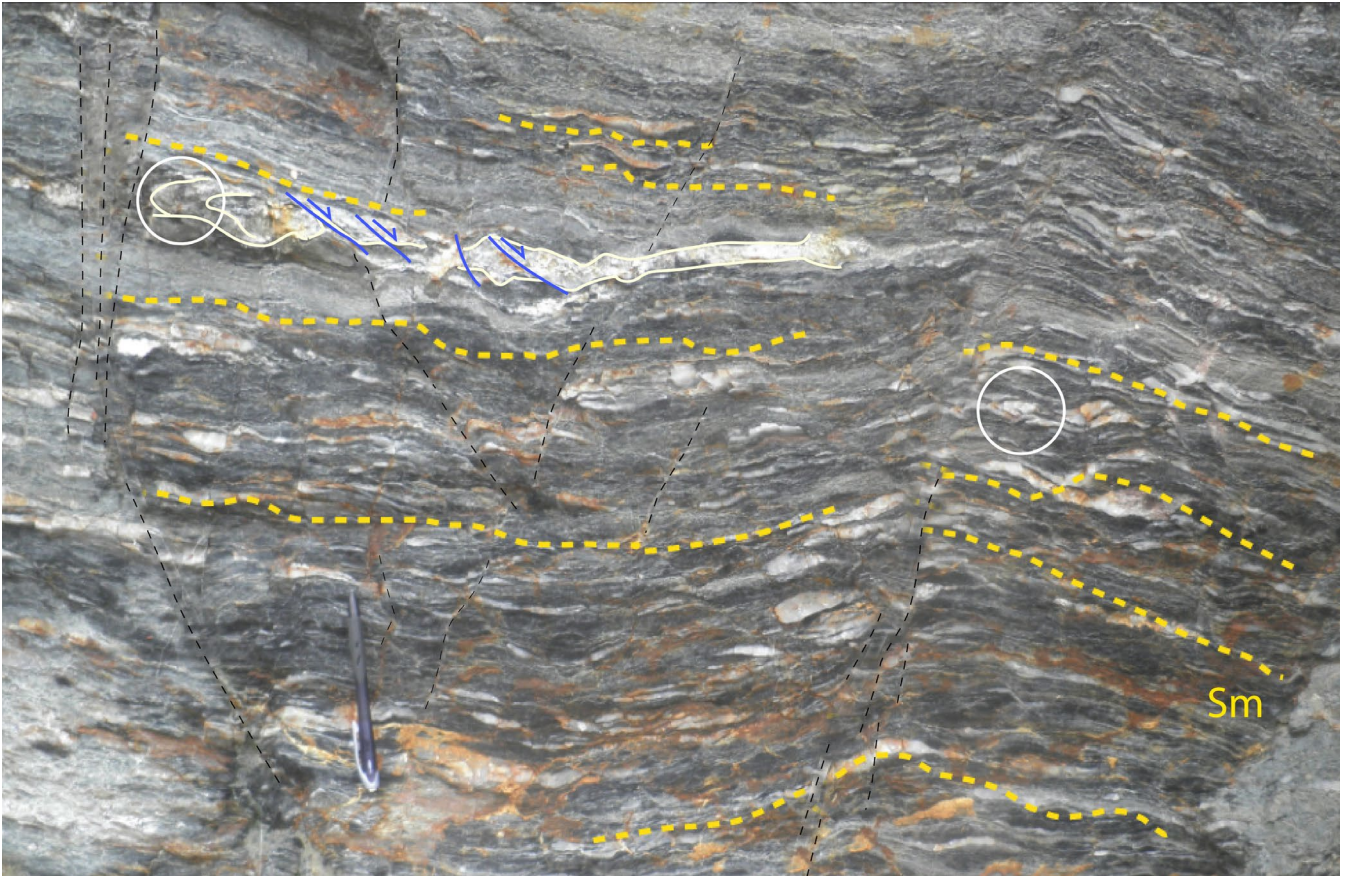


Figure 13. Intensely transposed mica-schist in the NMGS at the contact with the low-grade sequence (LGS) north of Zebra Bay. The schist shows disrupted and boudinaged quartz veins and occasional relict, isoclinal hinges in quartz veins (white circles). A thicker quartz vein (photo top left) shows segmentation and offset along small faults indicative of brittle, extensional boudinage in dextral shear. The small faults are shown by the blue line traces with hanging wall down sense. Transposition foliation Sm: yellow dashed lines. Sub-vertical, fine dashed black lines (photo left) are younger normal faults. (fig 3.4b, Mulder, 2013).

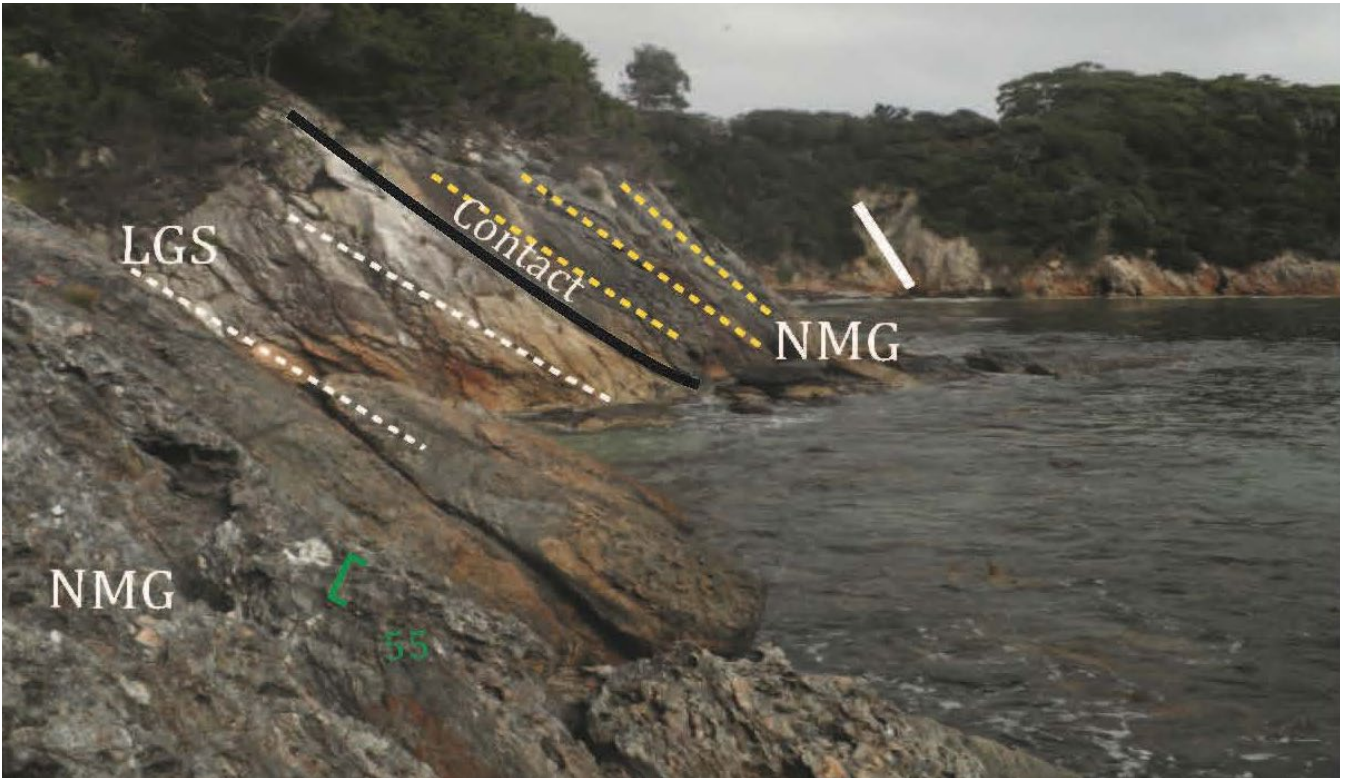


Figure 14. West-dipping contact between the underlying low-grade LGS quartzite units and the overlying NMG schist units (fig. 3.4c, Mulder, 2013). The view is looking south in coastal exposure on the east side of Cox Bight. So/Sm in the LGS (white dashed lines) is sub-parallel to Sm in the NMG (yellow dashed lines). The green strike/dip symbol indicates the Sm foliation has a 55° west dip. A north-west-dipping brittle fault is shown by the heavy white line in the bay in the distance. There is also a suggestion of gently west-dipping, west-over-east sense shear bands in the quartzite 1-2 m below the contact (see Figure 12b).

3.3 Structure of the Southern High-grade Belt (SMGS)

The northern margin of the southern high-grade belt (SMGS) is also an east-northeast-trending high strain zone that shows marked deflection of So/Sm into the Sm foliation at the contact with the SMGS schist (Figure 15). This was designated as D4 by Mulder (2013) and Mulder et al. (2015) therefore postdating the younger Devonian north-south trending open folds.

Without clear overprinting, apart from brittle -cataclastic zones grouped with D4, we propose that the high-strain zone (HSZ) contacts developed during LGS and SMGS juxtaposition, and were later reactivated with strong brittle overprints during 1) Late-Cambrian deformation and development of the Port Davey-Bathurst Harbour strike-slip basin, and 2) during the Devonian folding events.

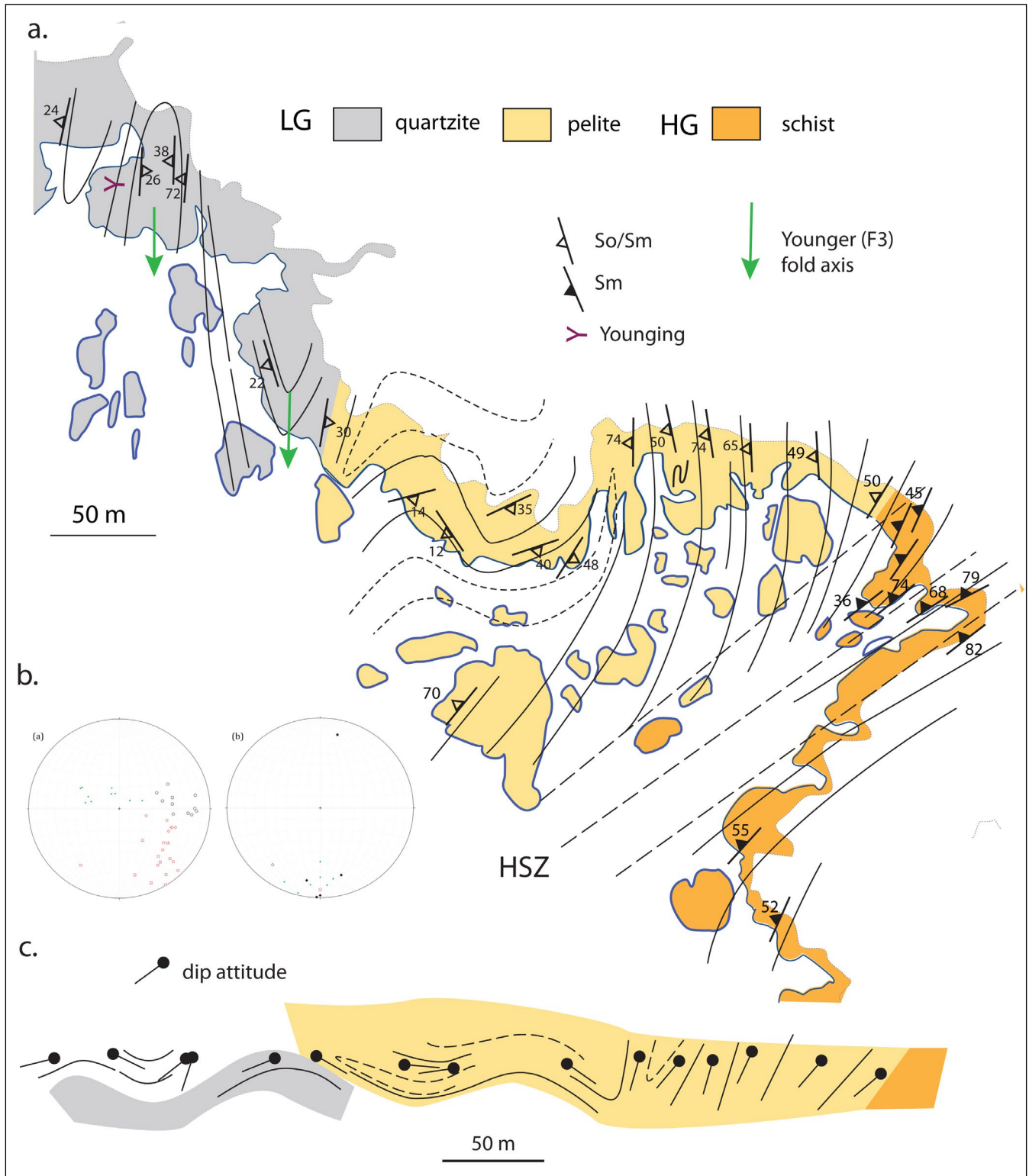


Figure 15. Structural relationships at Contact Cove. a) Structure and formline map of the coastal outcrops (fig. 3.7, Mulder, 2013). b) Stereonets of the structural data (fig. 3.11, Mulder, 2013). c) Approximate east-west structural profile across Contact Cove.

3.4 Linking the Structure of the NMGS and the SMGS

Utilising the detailed formline maps and coastal profiles A-A', C-C', D-D' and E-E' (Figure 16) a composite east-west structural profile was constructed in an attempt to define the regional structure and the links between the NMGS and the SMGS (Figure 16). The evolution of the final structural interpretation is shown by the changes from a stepped composite profile (Figure 16b), to a compressed profile that is positioned in the coastal region between Bridge Point and Contact Cove (Figure 16c), to a final schematic regional profile (Figure 16d).

The formline map (Figure 16a) shows north-south trending formlines through the low-grade pelite sequence (LGS) with swings or changes in strike approaching both contacts with the NMGS and the SMGS, due to re-activation as brittle-ductile zones (Mulder et al., 2015). The individual profiles (Figure 16b) largely reflect the younger, open north-south folds apart from the deflection at the contacts with the NMGS and SMGS. In profile there is an overall westerly dip across the LGS to give an asymmetric regional form. This is in contrast to the overall upright open geometry of the Red Point Hills folds.

The schematic profile (Figure 16d) is discussed further in Section 4. This interpreted profile is an oblique intersection with an inferred regional scale, inclined, west-plunging tight to isoclinal macro-fold. The younger, open north-south-trending Red Point Hills folds are superimposed on this early Cambrian regional fold.

4.0 REGIONAL MAP RELATIONSHIPS/INTERPRETATION

Based on the isoclinal folded nature of the Southern Tyennan domain (Gray & Vicary, 2022a) and the isoclinal fold-stack geometry of the West Coast high-grade coastal belt (Gray et al., 2022) the Red Point NMGS and SMGS outcrop belts have been re-interpreted as the limbs of an inclined plunging isoclinal macro-fold. This interpretation is presented in a series of figures Figure 17, 18 and 20. The structural data of Lennox (2013) and Mulder (2013) were utilised to explain the map pattern of litho-tectonic units, the younging data and the lineation pattern shown in Figure 5).

The structure of the Red Point Hills low-grade "pelite" belt is dominated by a series of younger, open generally south-plunging, north-south trending anticlines and synclines cut and offset by a series of sub-vertical east-west-trending faults that show apparent right lateral movement sense (Figure 17). South of the Ray River Fault the regional structure is dominated by the Red Point Hills Syncline-Anticline and the Louisa Point An-

ticline (green axial surface traces, Figures 17 and 18). The low-grade quartzite north of the Ray River fault shows formline-map patterns indicating complex re-folding with both east-west folds and northeast-trending folds (Figure 18).

Components of the fold-geometric model (Figure 20) are:

1. Macro-fold limbs are represented by the NMGS north-trending belt with generalised attitude of $200^{\circ}/45^{\circ}\text{W}$ (as western limb) and the SMGS north-east-trending belt with generalised attitude of $245^{\circ}/65^{\circ}\text{W}$ (as eastern limb) (Figure 17).
2. The apparent convergence of these limb segments in map view (Figure 17) give a β intersection of $43^{\circ}/270^{\circ}$ as the inferred Red Point macro-fold axis with an approximate reclined geometry (Figure 19). Combining all structural data in the MGS units gave a β intersection of $41^{\circ}/254^{\circ}$ (stereonet inset in Figure 20a).
3. Younging data from Lennox (2013) and Mulder (2013) suggest the western, structurally higher limb (the NMGS) is structurally overturned but with right-way-up younging, whereas the southeastern structurally lower limb (the SMGS) is upside down (Figure 17).
4. The axial surface trace (AST) of the macro-fold separates domains of right-way-up younging on the upper limb from upside younging beds on the lower limb (Figure 17).
5. Limited mineral lineation (Lm) data (Figure 18) suggest the upper limb has a generalised Lm of $40^{\circ}/310^{\circ}$, whereas Lm on the lower limb has a northeast-southwest trend. The only data available are attitudes of $\sim 30^{\circ}/035^{\circ}$ on the eastern limb of the Louisa Point Anticline. Removal of the younger folding gives a restored Lm trend of 032° and a calculated plunge of 50° (using apparent dip method on lower limb with attitude $240^{\circ}/65^{\circ}\text{W}$) (Figure 19).
6. Detailed sections (Figure 16) constructed using structure and younging data from Mulder (2013) suggest that the southern part of the hinge of the inferred Red Point macro-fold is not preserved in the low-grade (LGS) coastal exposures but is truncated by the Contact Cove D4 high strain zone of Mulder (2013). Younging data suggests the coastal sequence is right-way-up and therefore on the upper limb of the macro-fold.

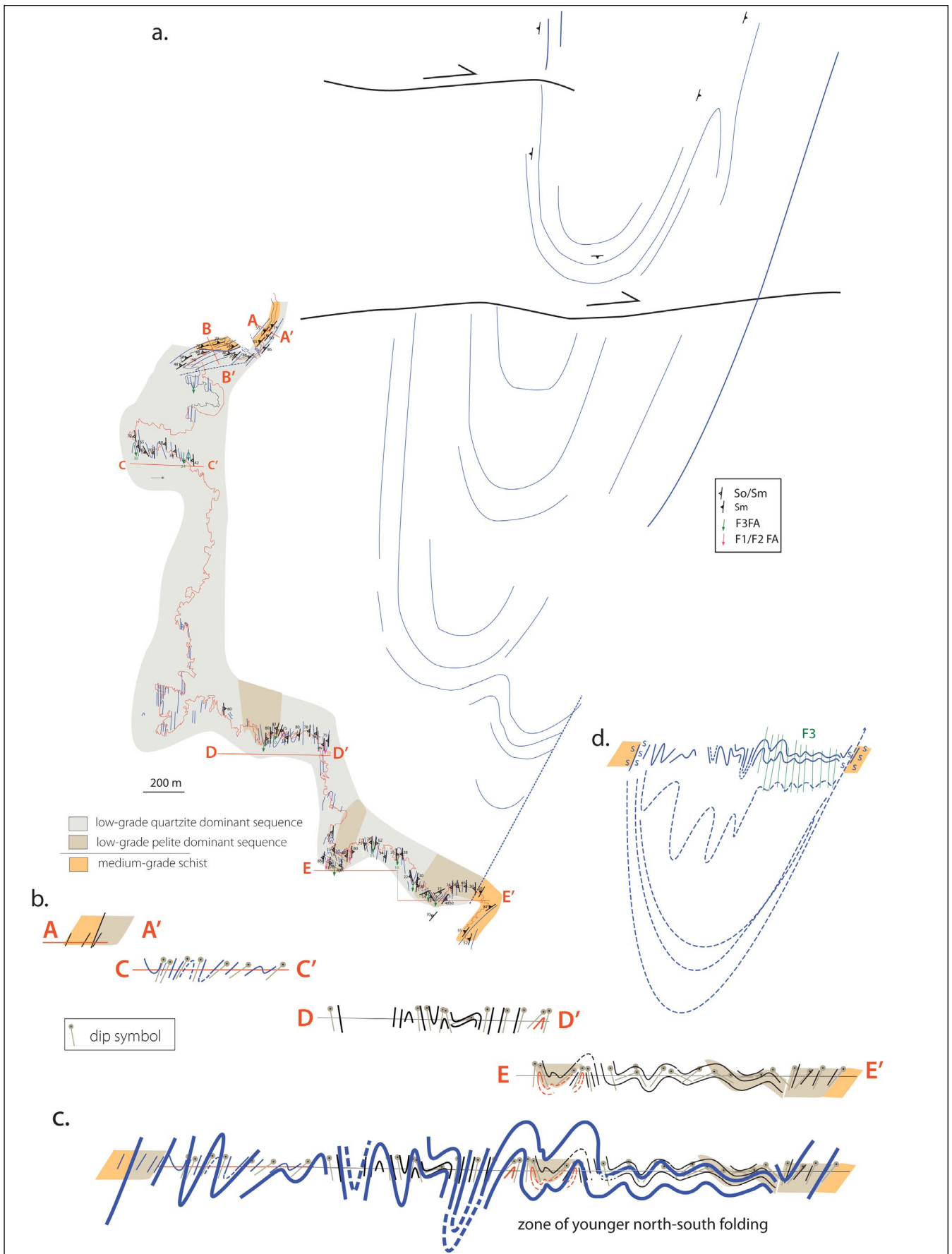


Figure 16. Cox Bight-Red Point coastal structure map and structural profiles based on data from Mulder (2013). a) Detailed structure and formline map with lithological base from Mulder (2013, fig.2.1). b) Composite structural profile made up of profiles from north to south of A-A' (Figure 12b), B-B' (Figure 12c), C-C', D-D' and E-E' (Figure 15c). c) Simplified geometric interpretation with anticlinal-synclinal form in the low-grade sequence (LGS) reflecting the Red Point Hills Anticline-Syncline pair. d) Overall geometric interpretation showing the younger anticline obliquely superimposed on the inferred west-plunging Red Point macro-fold.

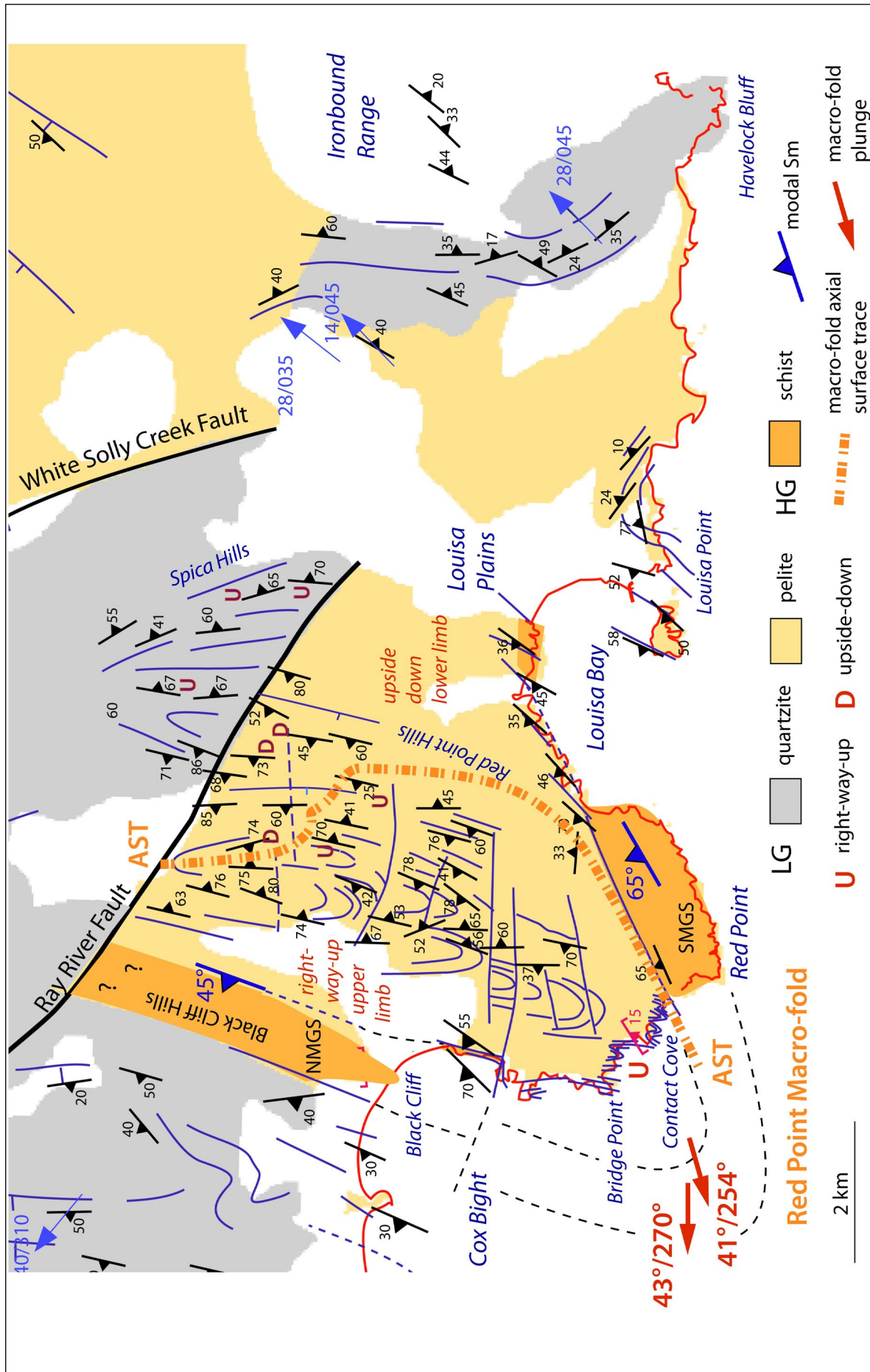


Figure 17. Structure map of the Red Point macro-fold incorporating data from Lennox (2013), Mulder (2013) and BHP mapping (Hall, 1965) north of Cox Bight. The macro-fold axial surface trace (AST) is shown by the dashed-dot orange trace. Younging data are shown by orange U (right-way-up) and pink D (upside down). Lineation Lm data (Hall, 1965) are shown by the blue arrows. The calculated β axis (macro-fold axis) is $43^\circ/270^\circ$ (see Figure 19) or $41^\circ/254^\circ$ (see Figure 20a).

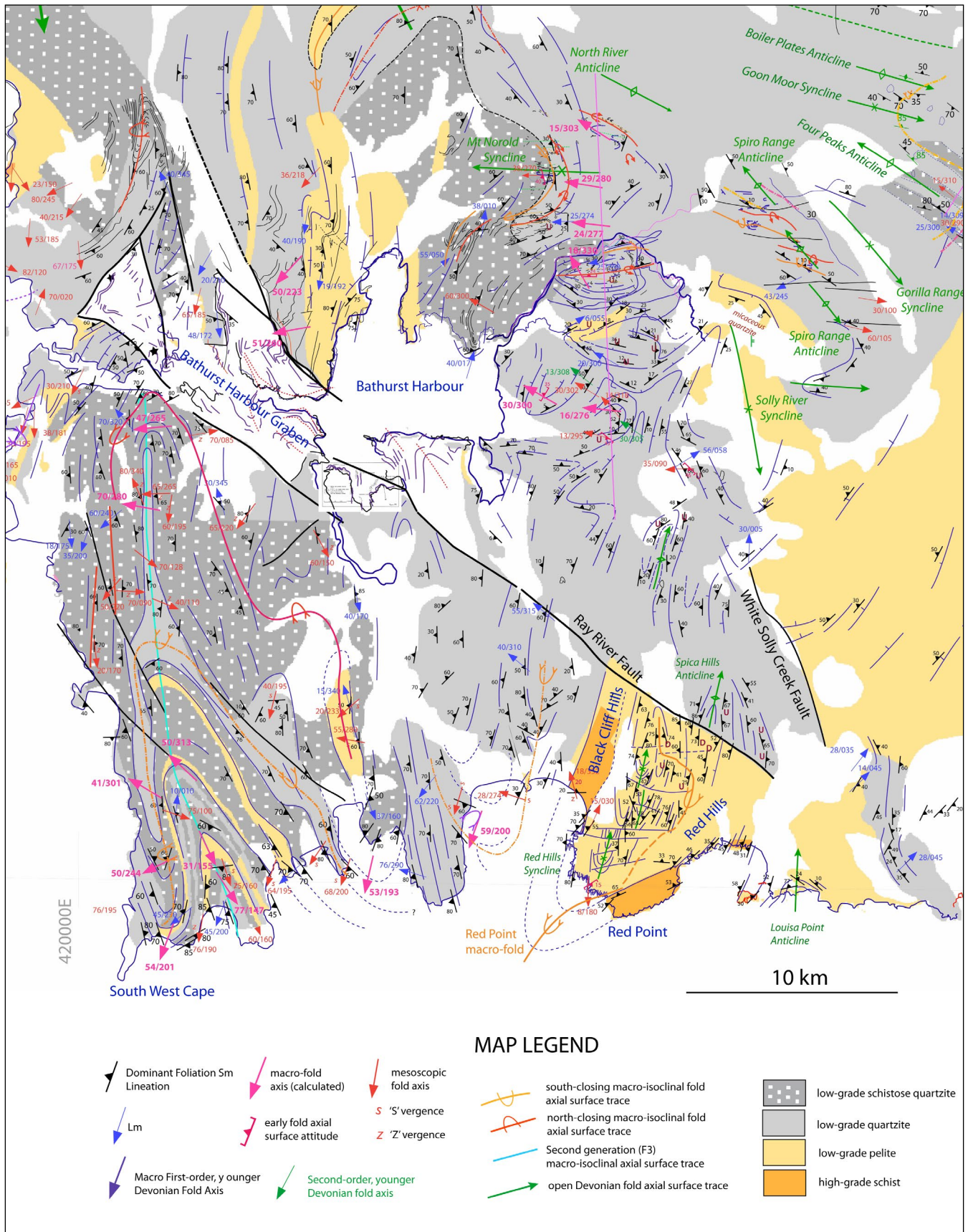


Figure 18. Regional structure map of the Harrys Bluff-High Round Mountain-Red Point Hills-Cox Bight-Louisa Bay area. Orange dashed-dot trace is the axial surface trace of the inferred Red Point macro-fold. Lineation data are shown by the blue arrows. Lithological map base is from Mineral Resources Tasmania 1:250,000 digital atlas series.

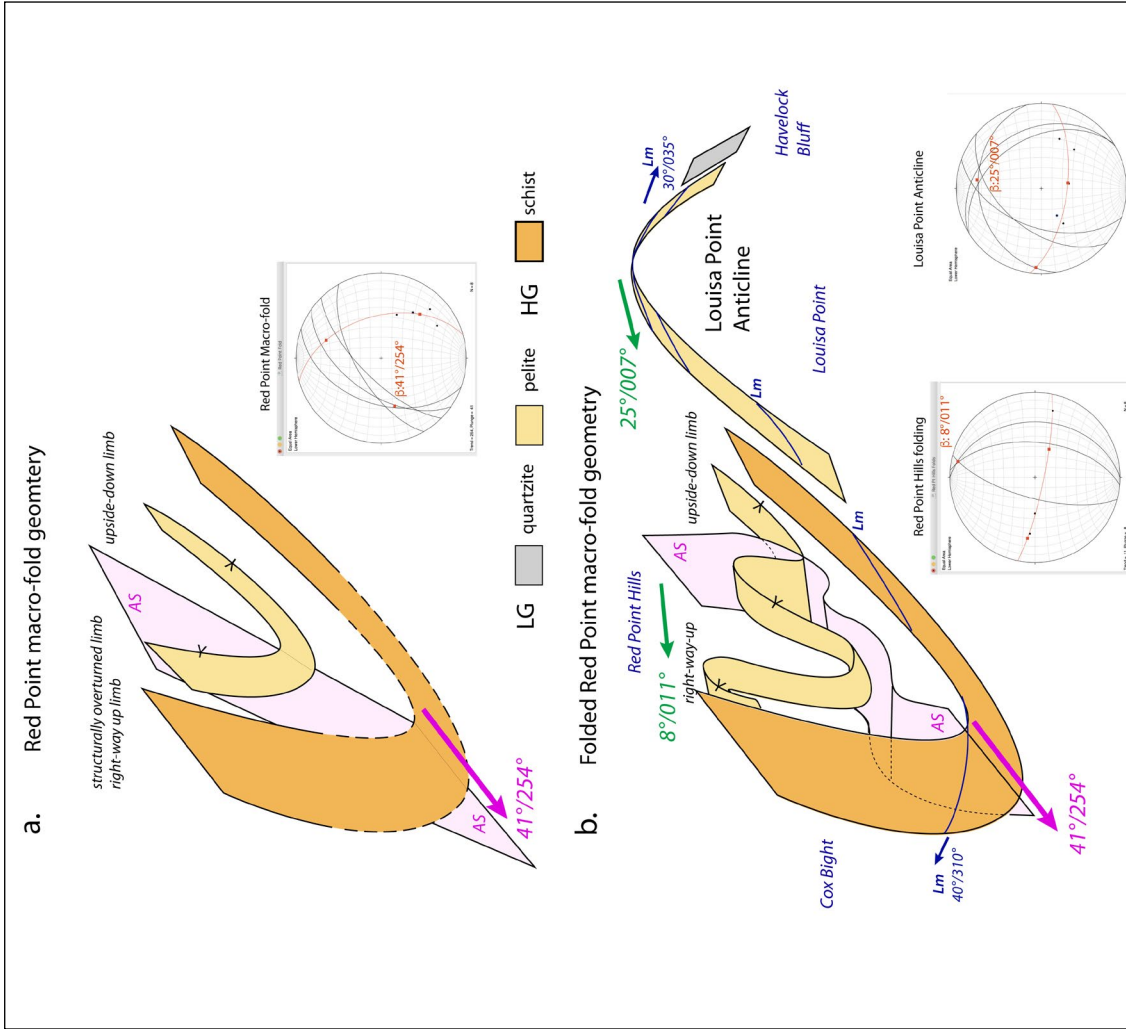


Figure 20. Interpretative 3D structural geometry of the Red Point Hills-Red Point area. a) Macro-fold form by connecting the northern and southern HG belts by an inclined plunging closure with a β axis of $41^\circ/254^\circ$. b) 3D schematic geometrical diagram of a refolded Red Point macro-fold by younger north-south folding in the Red Point Hills and the Louisa Bay-Louisa Point area. The east-west-trending, right lateral strike slip-faults have been removed in the 3D diagram. Stereonet insets show the β fold axis determinations for the Red Point Hills folding (β : $8^\circ/011^\circ$) and the Louisa Point Anticline (β : $25^\circ/007^\circ$).

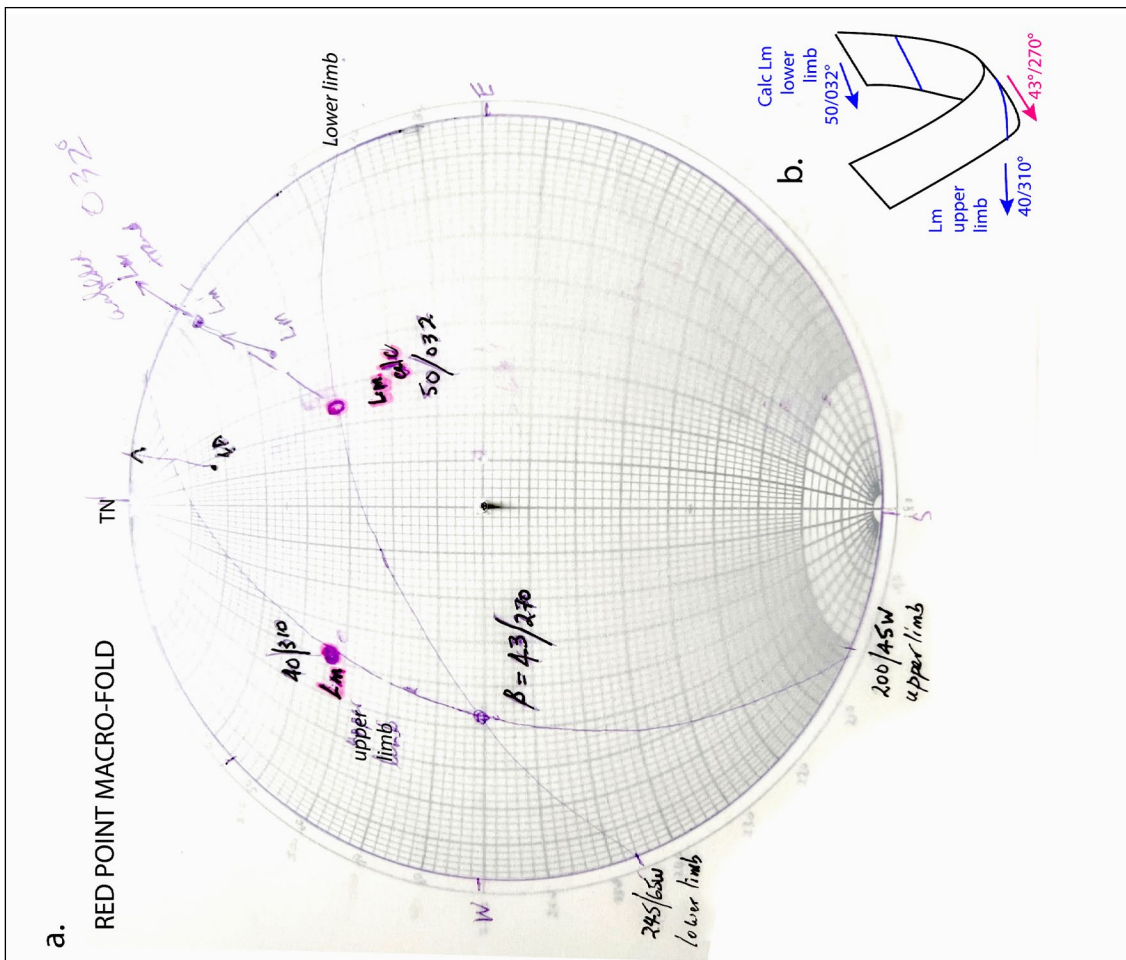


Figure 19. Stereographic projection plots of the upper and lower limbs of the inferred Red Point macro-fold with a β axis (macro-fold axis) of $43^\circ/270^\circ$ shown. Pink dots show the Lm lineation trends on these respective limbs. The upper limb Lm attitude is based on a measured lineation in quartzite north of Cox Bight, whereas the lower limb Lm is calculated as $50^\circ/032^\circ$ using Lennox (2013) data on the east limb of the Louisa Point Anticline. The plunge of the Louisa Point Anticline was removed to give the 032° trend of the restored lineation for the lower macro-fold limb.

5.0 EMPLACEMENT SHEAR SENSE AND TRANSPORT DIRECTION FOR THE RED POINT METAMORPHIC COMPLEX

A lack of measured shear band data from the Red Point Metamorphic Complex required attitude estimates of foliation (Sm) and shear bands (Sb) from the photographs in Mulder (2013) (Figure 14 and 21). These have provided approximate transport directions only. Analysis was undertaken on two localities in the NMG in Cox Bight (Figure 22a). Both data sets were restored with Sm rotated to the horizontal after removal of the younger Devonian fold plunge to give the restored Sb attitude and therefore the transport direction (Figure 22b).

1. NMG-LSG contact zone (Figures 12 and 14) with suspected west-over-east shear bands in quartzite below the contact (fig.3.4c, Mulder, 2013). Attitude estimates used are Sm 045/60NW and Sb 035/20NW giving a transport direction (TD) of 130°.
2. NMG-LSG contact zone (Figure 12) with sinistral shear band (fig.3.3c, Mulder, 2013) and north-east-over-west shear sense. Attitude estimates used are:
Sm: 070/15N (derived from Mulder map fig. 3.3)
Sb: 030/70NW
gave a transport direction (TD) of 296°.

Both datasets suggest a movement plane of 303°-123°. For discussion of shear sense determinations for the Southern Tyennan domain see Gray et al. (2022).

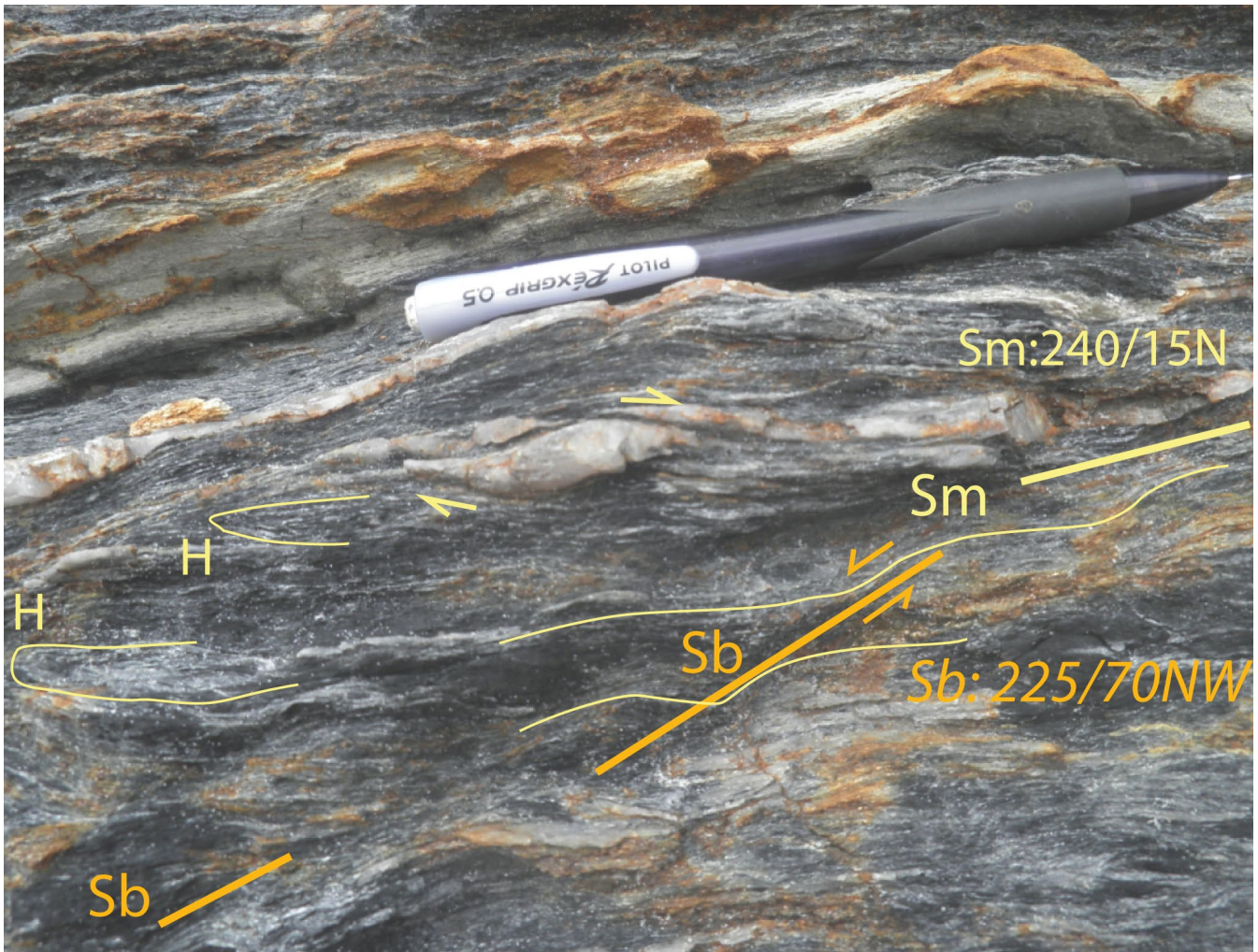


Figure 21. Shear sense indicators within intense Sm of the NMGS near the LGS contact (see Figure 12 for location). View is to the north showing dextral (top-to-the-east) asymmetric quartz fish within the Sm. Sinistral, east-over-west shear bands are also present, suggesting either reactivation of the contact high strain zone or development of an antithetic shear band set. Both indicators were designated as D4 by Mulder (2013).

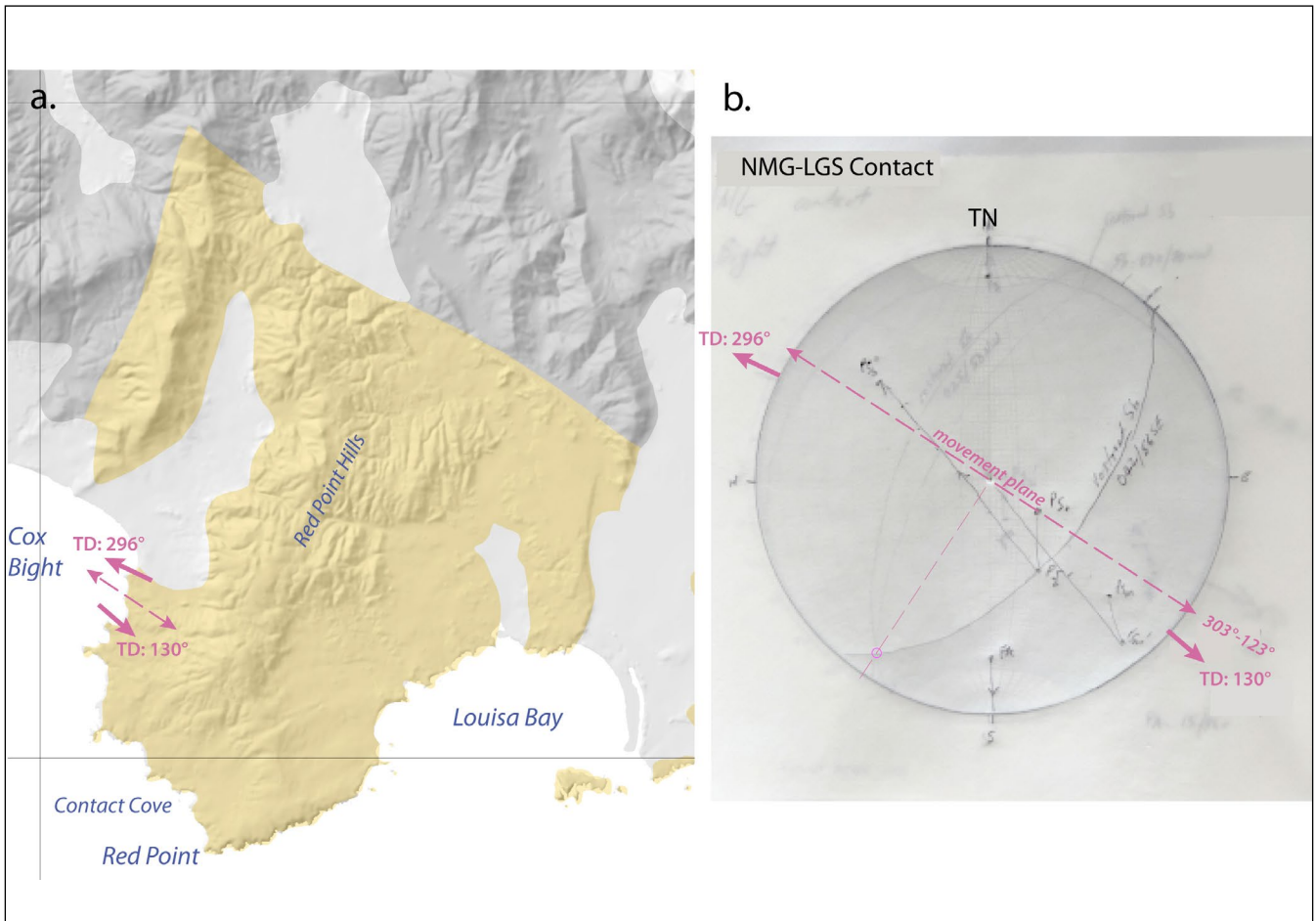


Figure 22. Transport directions for emplacement of the northern HG belt/sheet (NMGS) over the low-grade belt/sheet (LGS). a) Litho-tectonic unit drupe over the DEM showing the calculated transport directions from shear bands. b) Stereographic projection with superimposed stereonets of the restored shear band data.

6.0 SUMMARY AND CONCLUSIONS

The previous interpretation of the Red Point Metamorphic Complex was 1) a series of fault-bounded blocks cut by dextral high strain zones (HSZ) and dextral brittle faults (Mulder, 2013 and Mulder et al., 2015) and 2) the dominant folding in the coastal exposures was open north-south trending folds that match the Red Point Hills macro-folds.

This is in contrast to the macro-fold interpretation presented here. Given 1) the presence of regional scale isoclinal folds through the eastern part of the Southern Tyennan and 2) the apparent convergence of the NMG and SMG belts, they were treated as limb segments to reconstruct an early macro-fold closure approaching reclined geometry with a plunge of $43^\circ/270^\circ$ ($41^\circ/254^\circ$ for all data). The early macro-fold has been refolded, particularly the low-grade pelite sequence in the fold core, by the north-south-trending open folds that dominate the Red Point Hills (Figure 20). Both fold sets have

been offset by east-west-trending brittle faults and reactivated high-strain zones.

Unfolding the macro-fold indicates the ~1 km thick high-grade metamorphic sheet, made up of the NMG and SMG segments, is the structurally lowest unit in this part of the Southern Tyennan domain. The stacking order of litho-tectonic units is quartzite overlying low-grade pelite (LGS) overlying high-grade schist (MGS). Younging data indicates this sequence is upside down. Shear sense from shear bands near the NMGS-LGS contact give an overall movement plane of $303^\circ-123^\circ$ (Figure 22).

The Red Point macro-fold (element 7 in Figure 1) is interpreted to be the structurally lowest macro-fold in the Southern Tyennan domain (Gray and Vicary, 2022c). It sits below the South West Cape mega-sheath fold (element 5 in Figure 1) but above the isoclinal fold pair (element 6 in Figure 1) that dominates the eastern part of the Southern Tyennan domain (Gray and Vicary, 2022c).

7.0 ACKNOWLEDGMENTS

- Mineral Resources Tasmania (Andrew McNeill) for providing support through the 2016-2020 Geoscience Initiative, and reviewing the document.
- Chris Large for editing and formatting this Tasmanian Geological Survey publication.
- Parks and Wildlife Service (PWS) for allowing helicopter access and landing in the World Heritage Area as well as permits for measurement, sampling and photograph collection.
- Jason Bradbury NRE (Department of Natural Resources and Environment) for assistance with WHA and PWS permits for scientific research.
- Rodney Smith from Rotorlift for helicopter transport into the Tasmanian southwest.
- Rick Allmendinger and Nestor Cardozzo for use of OSX Stereonet.

8.0 REFERENCES

- Chmielowski, R.M. 2009. The Cambrian Metamorphic History of Tasmania. Unpublished PhD Thesis, The University of Tasmania.
- Gray, D.R. and Vicary, M. J., 2022a. Structural Geology of the Arthur Range, Central Tyennan Domain, Tasmania. Mineral Resources Tasmania, *Geological Survey Paper*, 8, 79p.
- Gray, D.R. and Vicary, M. J., 2022b. Mega-Sheath Fold Core of the Southern Tyennan Domain, Tasmania: The De Witt-Propsting and South West Cape Sheath Fold Systems. *Geological Survey Paper*, 10, 80p.
- Gray, D.R. and Vicary, M. J., 2022c. Structural Geology of the eastern Southern Tyennan Domain, Tasmania. Mineral Resources Tasmania, *Geological Survey Paper*, 11, 48p.
- Gray, D.R., Vicary, M. J. and McNeill, A.W., 2022. Structure of the High-grade Coastal Belt, Southern Tyennan Domain, Tasmania. Mineral Resources Tasmania, *Geological Survey Paper*, 9, 87p.
- Hall, W.D.M. 1965. Unpublished Progress Report No.1-March-June 1965 for Exploration Licence 13/65 Southwest Tasmania: Geological and geochemical exploration in the area between Bathurst Channel, Cox Bight and South West Cape. 68p. TCR 65-0398.
- Hall, W.D.M., McIntyre, M.I., Corbett, E.B., McGregor, P.W., Fenton, G.R., Arndt, C.D. and Bumstead, E.D. 1969. *Report on Field Work in Exploration Licence 13/65, South-West Tasmania During 1967-68 Field Season*. TCR 69_0555.
- Halpin, J.A., Jensen, T., McGoldrick, P., Meffre, S., Berry, R.F., Everard, J.L., Calver, C.R., Thompson, J., Goemann, K. and Whittaker, J.M. 2014. Authigenic monazite and detrital zircon dating from the Proterozoic Rocky Cape Group, Tasmania: Links to the Belt-Purcell Supergroup, North America. *Precambrian Research*, 250, 50-67.
- Lennox, P.G. 2013. Geology of parts of the Bathurst and Maatsuyker map sheets. Tasmanian Geological Survey Record 2013/03, 30p.
- Meffre, S., Berry, R.F. and Hall, M., 2000. Cambrian metamorphic complexes in Tasmania: Tectonic implications. *Australian Journal of Earth Sciences*, 47, 971-985.
- Mulder, J.A. 2013. The Structure and Metamorphism of the Cox Bight-Red Point Area, South West Tasmania. Unpublished Honours Thesis, The University of Tasmania. 76p.
- Mulder, J.A., Berry, R.F. and Scott, R.J. 2015. The structure and metamorphism of the Red Point Metamorphic Complex-- A newly discovered high-pressure metamorphic complex from the south coast of Tasmania. *Australian Journal of Earth Sciences*, 62, 969-983.
- Stefanski, M.Z. 1957a Progress Report on Regional Geological Survey of the Port Davey-Cox Bight Area. Tasmanian Department of Mines, *Technical Report*, 2, 87-106.
- Stefanski, M.Z. 1957b. Geological Compilation in the Bathurst Harbour Area. Unpublished Map, Mineral Resources Tasmania.
- Taylor, A.M., 1959. Precambrian Rocks of the Old River Area. Tasmanian Geological Survey, *Technical Report*, 4, 34-36.



Tasmanian
Government

Mineral Resources Tasmania

PO Box 56 Rosny Park

Tasmania Australia 7018

Ph: +61 3 6165 4800

info@mrt.tas.gov.au www.mrt.tas.gov.au